NUREG/CR-3444
BNL-NUREG-51699
Vol. 6

The Impact of LWR Decontaminations on Solidification, Waste Disposal and Associated Occupational Exposure

Prepared by P. Soo, C. R. Kempf, K. Brumfield,
L. W. Milian, J. W. Adams

Brookhaven National Laboratory

Prepared for
U.S. Nuclear Regulatory Commission

AVAILABILITY NOTICE

Availability of Reference Materials Cited in NRC Publications

Most documents cited in NRC publications will be available from one of the following sources:

1. The NRC Public Document Room, 2120 L Street, NW, Lower Level, Washington, DC 20555

2. The Superintendent of Documents, U.S. Government Printing Office, P.O. Box 37082, Washington, DC 20013-7082

3. The National Technical Information Service, Springfield, VA 22161

Although the listing that follows represents the majority of documents cited in NRC publications, it is not intended to be exhaustive.

Referenced documents available for inspection and copying for a fee from the NRC Public Document Room include NRC correspondence and internal NRC memoranda; NRC Office of Inspection and Enforcement bulletins, circulars, information notices, inspection and investigation notices; Licensee Event Reports; vendor reports and correspondence; Commission papers; and applicant and licensee documents and correspondence.

The following documents in the NUREG series are available for purchase from the GPO Sales Program: formal NRC staff and contractor reports, NRC-sponsored conference proceedings, and NRC booklets and brochures. Also available are Regulatory Guides, NRC regulations in the *Code of Federal Regulations*, and *Nuclear Regulatory Commission Issuances*.

Documents available from the National Technical Information Service include NUREG series reports and technical reports prepared by other federal agencies and reports prepared by the Atomic Energy Commission, forerunner agency to the Nuclear Regulatory Commission.

Documents available from public and special technical libraries include all open literature items, such as books, journal and periodical articles, and transactions. *Federal Register* notices, federal and state legislation, and congressional reports can usually be obtained from these libraries.

Documents such as theses, dissertations, foreign reports and translations, and non-NRC conference proceedings are available for purchase from the organization sponsoring the publication cited.

Single copies of NRC draft reports are available free, to the extent of supply, upon written request to the Office of Information Resources Management, Distribution Section, U.S. Nuclear Regulatory Commission, Washington, DC 20555.

Copies of industry codes and standards used in a substantive manner in the NRC regulatory process are maintained at the NRC Library, 7920 Norfolk Avenue, Bethesda, Maryland, and are available there for reference use by the public. Codes and standards are usually copyrighted and may be purchased from the originating organization or, if they are American National Standards, from the American National Standards Institute, 1430 Broadway, New York, NY 10018.

NUREG/CR-3444
BNL-NUREG-51699
Vol. 6
RW

The Impact of LWR Decontaminations on Solidification, Waste Disposal and Associated Occupational Exposure

Manuscript Completed: June 1989
Date Published: November 1989

Prepared by
P. Soo, C. R. Kempf, K. Brumfield,
L. W. Milian, J. W. Adams

Brookhaven National Laboratory
Upton, NY 11973

Prepared for
Division of Engineering
Office of Nuclear Regulatory Research
U.S. Nuclear Regulatory Commission
Washington, DC 20555
NRC FIN A3246

ABSTRACT

Studies were carried out to investigate if simulated decontamination reagent/resin waste combinations could give rise to thermal excursions during dewatering events. The results of temperature measurements and visual observations are given. In addition, the corrosion of various container materials in simulated decontamination resin waste was studied. In particular, the effects of gamma irradiation were quantified.

CONTENTS

LIST OF FIGURES

LIST OF FIGURES (Cont'd)

LIST OF TABLES

ACKNOWLEDGEMENTS

The authors gratefully acknowledge the assistance of A. Lopez and Vicki Feldman, Craig Sirot, Terry Jones and Madeline Batsche of the Technical Publishing Center for their skills in preparing the manuscript.

EXECUTIVE SUMMARY

Two different studies have been carried out this year, one involves an investigation to determine if thermal excursions or gas generation could be induced in ion-exchange resins which were reacted with simulated decontamination reagent/waste combinations. This research investigates the potential causes of such incidents which have occurred in resin wastes during processing and containerization. The second study was carried out to determine corrosion failure mechanisms for a range of container materials during long term exposure to decontamination reagents and gamma radiation.

Resin/Reagent Reaction Studies

Some preliminary experiments were conducted to first characterize various resins/reagent combinations, after which more detailed investigations were performed to measure temperature changes and to observe any other signs of chemical reaction such as smoke generation, color change, precipitation, etc.

Both anion exchange resin (IRN-78 and IONAC A-365) and cation exchange resins were studied. The former were loaded picolinic acid or EDTA (ethylenediamine-tetracetic acid) and the latter with $FeSO_4$. Loadings were at the 50 or 100 percent theoretical limit. For the main tests the resins were placed in a Buchner funnel and reacted with 3M nitric acid and ~0.8N potassium permanganate. Resins were in the oven-dried form or in a wet vacuum-aspirated condition.

Oven-dried anion resin loaded with picolinic acid showed temperature increases of up to about 15°C with the addition of 7-9 mL of nitric acid. In a few cases, smoke accompanied the reaction, but no significant signs of major chemical changes were noted. When potassium permanganate was later added to the resin/acid mixture, after the temperature had decreased to ambient, no additional temperature changes were observed. However, during vacuum aspiration of the resin/acid/permanganate mixture, a vapor cloud was usually formed as reagent was removed from the resins by the flowing air. It seems that the vapor is a frozen aerosol of reagent which causes a drop in temperature in the flask that was used to collect the moisture from the resin.

Similar results were obtained for oven-dried anion resins loaded with EDTA.

When the experiments were repeated for vacuum-aspirated anion resin, there were only modest increases in temperature when nitric acid was added. No temperature changes were found when permanganate was subsequently added. During additions of the two reagents, smoke was not observed, but vapor clouds were noted during aspiration.

It is concluded that the thermal excursions observed for the anion resins are caused by resin hydration processes. No chemical reactions between the resins and the nitric acid and permanganate appear to be involved.

Limited studies on cation resins loaded with ferrous ion show basically similar behavior to the anion resins. Nitric acid causes a temperature increase for oven-dried resins only. Subsequent additions of permanganate had no effect.

In summary, the only thermal excursions observed for the current resin/reagent contaminations occurred for oven-dried resins. These resulted from hydration effects. Since resin wastes generated in industry are usually in a wet or moist state, thermal excursions and gas generation for systems similar to the ones evaluated in the program will not likely occur during processing and storage. This work supports the hypothesis that the several events that occurred in the past were connected with contamination of the resins and that this possibly led to biodegradation and gas generation [Bowerman and Piciulo, 1986].

Corrosion of Waste Container Materials

This task was initiated to evaluate the compatibility of a range of container materials with a simulated decontamination resin waste. The materials include Ferralium 255 (a duplex stainless steel), TiCode-12 (a dilute titanium alloy), Types 304 and 316 stainless steel, carbon steel, and high-density polyethylene. The carbon steel coupons were added after the first irradiation cycle when some of the original specimens were deemed surplus and removed to provide space. Thus, the carbon steel specimens were exposed to resins which had been pre-irradiated to approximately 5×10^7 rad.

To check how corrosion is influenced by gamma irradiation (which is present in most types of low level waste) and by the presence of organic reagents on the resin, four types of corrosion test were initiated:

a) corrosion in mixed-bed resins with the anion component loaded with picolinate/formate; cation resin in the H^+ form;

b) corrosion in as-received mixed-bed resins (i.e., anion resin in the hydroxide; cation resin in the H^+ form;

c) similar to (a) but in the presence of a gamma field of about 1×10^4 rad/h; and

d) similar to (b) but in the presence of a gamma field of about 2×10^4 rad/h.

The four resin beds were contained in glass liners measuring 7.0 cm ID × 30.5 cm in height. The metallic specimens were placed horizontally in the resins in two layers, one resting on the flat base of the glass liner and the other close to the resin surface.

The high density polyethylene (Marlex CL-100) specimens were made from strips measuring 10.2 × 1.25 × 0.32 cm. They were bent into a "U-bend" configuration by bending them and fastening the two ends with steel nuts and bolts. In the molding of the drum from which the specimens were cut, one side of the drum becomes oxidized by air. When the oxidized material is on the outer surface of a U-bend specimen, cracks are formed because of the lower ductility. When the non-oxidized material is on the outer bend surface, no cracking is present. Crack propagation during testing was studied for samples with both oxidized (cracked) surfaces and non-oxidized (uncracked) surfaces on the U-bend specimens. The polyethylene specimens were placed between the two metallic specimen layers with the apex of each U-bend facing upward.

For the two systems being irradiated, the glass liners containing the resins and specimens were enclosed in sealed stainless steel pressure vessels connected to a pressure gauge/data logger system. A vacuum system was also connected to the vessel to facilitate purging and the removal of gas samples for analysis.

For the unirradiated tests, the liners containing the specimens were sealed with plastic foil and placed in a refrigerator at 10°C, the gamma irradiation temperature.

The table below summarizes the results of the corrosion studies.

Summary of corrosion results for container materials exposed to LOMI decontamination reagent and gamma radiation

Material	Control Resin		LOMI-Loaded Resin	
	Unirradiated	Irradiated	Unirradiated	Irradiated
Carbon Steel	Local pock mark attack during 68 d exposure; additional attack during next 216 d but at slower rate.	Local pock mark attack after 129 d irrad. to 6.2×10^7 rad; additional slower attack during cumulative irrad. of 344 d to 1.65×10^8 rad.	Local pock mark attack during 208 d exposure.	Local pock mark attack during 208 d irrad. to 5×10^7 rad.
T304 SS	No attack during 488 d exposure.	Spot attack during 447 d irrad. to 2.1×10^8 rad.	No attack during 412 d exposure.	Spot attack during 412 d irrad. to 1×10^8 rad.
T316 SS	No attack during 488 d exposure.	No attack during 447 d irrad. to 2.1×10^8 rad.	No attack during 412 d exposure.	Spot attack during 412 d irrad. to 1×10^8 rad.
Ti-12	No attack during 488 d exposure.	No attack during 447 d irrad. to 2.1×10^8 rad.	No attack during 412 d exposure.	No attack during 412 d irrad. to 1×10^8 rad.
Fe-255	No attack during 488 d exposure.	No attack during 447 d irrad. to 2.1×10^8 rad.	No attack during 412 d exposure.	No attack during 412 d irrad. to 1×10^8 rad.
HDPE	Some crack initiation and propagation during 488 d exposure.	No significant crack growth during 447 d irrad. to 2.1×10^8 rad.	Some crack initiation and propagation during 412 d exposure.	No significant crack growth during 412 d irrad. to 1×10^8 rad.

Carbon steel was attacked under all test conditions. There was no clear correlation between the presence of LOMI reagent and irradiation on the extent of attack. However, it was found that for all test conditions, the rate of initiation of corrosion "pock marks" with each test cycle tended to decrease. This could be connected with evaporation of moisture from the resins during testing and examination. Neither Type 304 nor Type 316 stainless steel suffered corrosion in the absence of irradiation. The presence of LOMI reagent did not make any difference for this non-irradiated condition. For the irradiated state, however, Type 316 stainless steel showed improved resistance to corrosion. This may be seen for as-received resins exposed to a gamma dose of 2.1×10^8 rad over a period of 447 d. Under these conditions, spot attack was noted for Type 304, but not for Type 316. If LOMI reagent was present on the resin, then both Type 304 and Type 316 showed spot attack after a 412 d irradiation to 1×10^8 rad. It seems clear that LOMI reagent encourages attack, at least for Type 316 stainless steel, since in this case the cumulative gamma dose was only 1×10^8 rad.

TiCode-12 and Ferralium-255 are superior to all of the other metal specimens in terms of corrosion resistance. Neither showed attack under any of the test conditions studied.

Finally, high-density polyethylene did not show crack initiation or propagation in a gamma irradiation environment because of the rapid loss of oxygen to resin oxidation processes. This lack of oxygen is known to greatly retard oxidative degradation of polymers. When irradiation is absent, then sufficient oxygen remains in the test system to allow some crack initiation and propagation in both as-received and LOMI-loaded resins.

1. INTRODUCTION

Chemical decontamination of light water reactor systems has been developed into an economically and technologically viable means of reducing radiation levels in commercial power plants. Components in the primary system become radioactively contaminated by deposition of corrosion products which are transported from the core region by the coolant. The often high radiation levels which result from this accumulated material can be effectively reduced by chemical dissolution.

The decontamination reagents used to effect this dissolution contain proprietary mixtures of chelating agents, buffers, and/or corrosion inhibitors, and are typically categorized as concentrated (reagent concentrations in the range of 2 to 5 percent) or dilute processes (concentrations of less than 2 percent). These reagents can be used in either fill-and-drain or feed-and-bleed modes and are often preceded by treatments to change the ionic form of species being removed to more soluble forms. The exhausted reagent may be regenerated by a cation exchange process which retains solubilized cations and radionuclides. Following completion of the decontamination, the organic acids in the reagents are typically removed by anion exchange resins which also help remove residual contaminants from the aqueous solution.

The wastes resulting from these processes consist of anion exchange resins, partially or perhaps fully expended with polyvalent anions from the decontamination reagent (i.e., organic acids), or components of oxidizing or reducing agents from the pretreatment solutions (e.g., NO_3^- or oxalic acid). Cation exchange resins may be partially to fully expended with solubilized corrosion products (primarily Fe^{2+}), complexed cations (e.g., Fe^{2+}-EDTA, or other ions from the process water (e.g., Mn^{2+} or Cu^{2+}). The anion resin wastes may be handled alone as they contain the majority of the chelates found in decontamination waste, or mixed with cation resins to dilute the radioactive concentration of the cation resin waste stream.

To meet the regulatory requirement of 10CFR Part 61 for shallow land burial, the dewatered resin wastes must either be packaged in approved high-integrity containers, or solidified in a manner such that the structural stability requirements specified in the NRC Technical Position on Waste Form [NRC, 1983] are met. Lack of stability of low-level waste in a shallow-land burial trench may lead to trench subsidence, enhanced water infiltration and waste leaching, which could result in accelerated transport of radionuclides with complexing agents used for decontamination. The degree to which these agents inhibit the normal sorptive capacity of the soil is dependent on the type of complexing agent, the radionuclide of concern, the soil properties, and whether the nuclide is present as a complex or is already sorbed to the soil.

Since Fiscal Year 1983, NRC has sponsored a program at Brookhaven National Laboratory (BNL) to determine if chemical decontamination wastes can be treated at the plant in a manner that will mitigate the potential hazards associated with disposal of these wastes (FIN A-3246). The first annual report [Davis, 1983], evaluated potential decontamination processes, the wastes generated and potential waste management practices. Follow-

ing that review, a test program was initiated to evaluate the effectiveness of incineration, acid digestion, and wet-air oxidation for degrading selected decontamination wastes. In addition, the program set out to assess the acceptability of solidified decontamination wastes for disposal in shallow land burial [Davis, 1985; Piciulo and others, 1985; Piciulo and Adams, 1986]. This work has included a laboratory evaluation of the solidification of dilute process decontamination wastes. Simulated decontamination resin wastes were solidified in cement and vinyl ester-styrene. Waste forms were examined for the presence of free liquid and were tested for mechanical durability and the ability to withstand immersion in water. During Fiscal Year 1986, work on the solidification of simulated chemical decontamination wastes was extended to include bitumen (asphalt) as a solidification agent. Last fiscal year, work was conducted on the effects of thermal cycling of simulated decontamination wastes resins solidified in cement and vinyl ester-styrene. Strength measurements were made to check the degree of degradation [Adams and Soo, 1988]. In addition, some tests were started to assess the corrosivity of simulated decontamination resin wastes to a range of container materials. Although dewatered unsolidified decontamination waste resins are not permitted at Barnwell, SC, they can be buried at Hanford, Washington, provided they are stabilized in a suitable way, such as containment in a high-integrity container.

During this fiscal year, work has been focused on two tasks. The main emphasis has been on the determination of chemical and physical conditions which could lead to thermal excursions, gas generation, and/or general degradation of waste ion-exchange resins used for clean-up at nuclear power plants. This task was initiated as a consequence of concern about three anomalous incidents. These were: a thermal excursion in resins undergoing dewatering at Arkansas Nuclear One (sufficient heat was produced to bring the temperature of the wastes to at least 365°F); and two gas generation/pressurization events in resin wastes undergoing transportation from Millstone Nuclear Station and from the James A. Fitzpatrick Nuclear Power Plant (gas pressures in the wastes were sufficient to result in the lifting of the lid of the shipping cask in both cases). In all three cases, resin wastes were involved and the dewatering process had been (or, in the case of the thermal excursion wastes, was in the process of being) performed. The resin wastes were quite heterogeneous and had not been thoroughly characterized. The specific causes of these events have not been identified.

This work will provide information to allow determination of whether such events could happen in the future, either during storage or processing at the plant, during transportation, or at the final disposal site. The plan for this task has involved setting up a simplified experimental system in which heat and/or gas generation as well as color changes, precipitates or other signs of chemical reaction can be observed. Specifically, IRN-78 and IONAC A-365 anion and IRN-77 cation resin batches were regenerated and their moisture contents in regenerated form were determined. Then, these resins were "loaded" with typical reagents or species that would be expected to be trapped on the resins from a decontamination campaign; for anion resins, picolinic acid and EDTA were used, while for cation resins, ferrous ions were used. The equilibrium moisture contents of these loaded resin forms were also determined.

Once batches of regenerated and decontamination reagent-loaded (or, in the case of the cation resins, metal ion-loaded) resins had been prepared, they were subjected to addition of oxidizing chemicals, in particular nitric acid and potassium permanganate solution. These additions were carried out in several ways: (1) in small increments coupled with monitoring of changes in pH of the resin slurry to allow observation of the exchange with nitrate and with permanganate for the regenerated form of the anion resins; (2) dropwise and in bulk to allow observation of the effect of oxidizing agent volume and also of the heat generation and absorbance taking place in the resin slurry; (3) with intermittent dewatering by vacuum aspiration between additions of nitric acid and potassium permanganate to simulate the dewatering which was known to have occurred in the heat and gas generating incidents described earlier. The results of these tests are given below in Section 2.

The second area of research was on the container corrosion program initiated last year. It is a small scale effort involving periodic inspection of container materials that have been exposed to simulated resin wastes and gamma radiation. Comparisons were made with as-received non-irradiated resins to determine the effects of decontamination reagents and radiation. This work is described in Section 3

2. DEGRADATION OF ION-EXCHANGE RESINS

A number of unexplained incidents involving organic ion exchange resins that had been used as part of clean-up systems at nuclear power plants have prompted research into the physical and chemical behavior of such resins in conditions analogous to those where the incidents took place. Heat and gas generation were observed.

The first incident occurred at Arkansas Nuclear One, January 1983, when ion exchange resins were being dewatered prior to disposal. In this incident, an exothermic reaction was initiated causing the resin wastes to become heated and causing smoke and/or steam to be given off. The other two events involved pressurization in containers of dewatered filter media from the Millstone Nuclear Station and the James A. Fitzpatrick Nuclear Power Plant [Bowerman and Piciulo, 1986].

The actual causes of these events were not identified. A review of the events was performed and several contributing factors were suggested based on the analytical information available from the waste generators or handlers and on a literature review of chemical and physical reactions or changes ion exchange resins may be subject to which could lead to heat generation and/or gas generation. This information forms the basis of the current research effort.

The purpose of this work is to determine chemical and physical conditions for ion exchange resins which could lead to thermal excursions, gas generation, and degradation of waste. It is hoped that the results of this study will help prevent future occurrence of potentially dangerous chemical reactions of radioactive resins.

2.1 Ion Exchange Resin Characteristics [Helfferich, 1962]

Ion exchangers are generally insoluble materials which carry exchangeable cations or anions. Those exchangers that are capable of exchanging cations are called cation exchangers, and those that are capable of exchanging anions, anion exchangers. Some materials are capable of exchanging both cations and anions. These are called amphoteric ion exchangers.

Not only do ion exchangers have the ability to exchange cations and anions, they also have the unique ability to regenerate themselves. If an exchanger has traded its original counter ion population, it can easily obtain these ions again. This can be done by placing the exchanger in a solution containing the original ions. The ions in turn attach themselves to the exchanger and the exchanger is reconverted to the original form.

The reversibility and other properties of ion exchangers can in part be explained by their structure. They consist of a framework with fixed electric charges and mobile counter ions. Counter ions are ions of opposite sign that move within the resin framework and can be exchanged.

Even though this general structure is common to all ion exchangers, it is their differences in behavior that separate them. Ion exchangers can be organic ion exchange

resins, ion exchange coals, mineral ion exchangers, and synthetic inorganic ion exchangers. They can exist in either gel, powdered, or bead form.

Organic ion exchange resins are widely used for waste water treatment in general and for decontamination at nuclear power plants in particular. Their matrix consists of an elastic three-dimensional network of hydrocarbon chains which carry fixed ionic groups. Many organic ion exchange resins have polyacrylic, poly-epoxyamine, or polystyrene backbone structures.

The structure, degree of crosslinking, and nature and number of fixed ionic groups in resins play a very important role in the ion exchange behavior and chemical, thermal, and mechanical stability of ion exchange resins. The degree of crosslinking determines the width of the matrix, the swelling ability of the resin, and the mobilities of the counter ions in the resin.

The chemical and thermal stability of resins is not unlimited. Chemical and thermal degradation of the matrix are the frequent causes of resin deterioration. This is sometimes caused by oxidation, loss of fixed ionic groups, and thermal hydrolysis.

The ion exchange behavior of the resins is chiefly determined by the fixed ionic groups (functional groups). The number of groups determines the ion exchange capacity. The nature of the fixed ionic groups affects the selectivity of the resins, and their specific chemical behavior under system conditions affects ion exchange equilibria.

Ion exchange resins used in nuclear power plant clean-up systems may be in a variety of "loading" forms; i.e., their counter ions could be H^+ or Fe^{+2} for cation resins, or OH^-, ethylenediaminetetraacetic acid) EDTA, nitrate, picolinate, permanganate, etc., for anion resins. In this research program an attempt has been made to simulate some of the chemical and physical conditions of the resins at the time they underwent the reactions mentioned earlier. Therefore, an effort has been made to study the effects and extent of loading of different ions on resins, the pH changes that result, and also to determine the moisture content and dewatering characteristics for different resins with different ionic loadings.

2.2 Preliminary Experiments

A few scoping experiments were initially performed to specify optimum resin preparation procedures and test equipment. Later, more comprehensive tests were conducted and are described in Section 2.3.

2.2.1 Materials

The resins used in these experiments were Rohm and Haas IRN-78 (anion resin, received in the hydroxide ion form), IRN-77 (cation resin, received in the hydrogen ion form), and Sybron IONAC A-365 (anion resin, received in the hydroxide ion form). The principal characteristics of these resins are listed in Table 2.1.

Table 2.1

Ion-exchange resin data from Rohm and Haas Company (Amberlite Ion Exchange Resin Laboratory Guide, March 1977)

Type of Resin (matrix material)	Functional Group Structure	Form (Physical)	Particle Size (mm)	Moisture Content (%)	pH Range	Total Capacity (meq/gm)[a] (dry weight)
IRN-77 (styrene-divinylbenzene)	R_2SO_3	Spherical beads	0.47–0.62	44–48	0–14	5.0
IRN-78 (styrene-(divinylbenzene)	R_2NR_3	Spherical beads	0.38–0.45	42–48	0–14	4.3
IONAC-A365 (polyacrylate)	R_2NR_2	Spherical beads	0.3–1.2	54–59	0–14	9.5

[a]See Appendix A.

The reagents used were NaOH, HCl, HNO_3, $KMnO_4$, $FeSO_4 \cdot 7H_2O$ (all manufactured by Mallinckrodt/Analytical grade), $Na_2C_2O_4$ (MCB/Powder), disodium ethylenediaminetetraacetic acid (Na-EDTA) (Aldrich/Analytical grade), picolinic acid (PA) (Aldrich/Analytic grade) and deionized water.

The solutions were made as follows:

(a) 1N NaOH—40 grams of NaOH were dissolved in deionized water to make 1L.

(b) 1N HCl—83ml of concentrated HCl were dissolved in deionized water to make 1L.

0.9F H_2SO_4—48.2ml of concentrated H_2SO_4 were dissolved in deionized water to make 1L.

(c) 0.5M HNO_3—50ml of 1M HNO_3 were dissolved in deionized water to make 100ml.

1M HNO_3—64ml of concentrated HNO_3 were dissolved in deionized water to make 1L.

3M HNO_3—192ml of concentrated HNO_3 were dissolved in deionized water to make 1L.

(d) ~0.8N $KMnO_4$—a super-saturated $KMnO_4$ solution was initially prepared by dissolution of an excess of $KMnO_4$ and heating. This solution was then standardized using the primary standard sodium oxalate ($Na_2C_2O_4$) which reacts as shown below (Kennedy, 1984):

$$5\ C_2O_4^{-2} + 2\ MnO_4^{-} + 16\ H_3O^{+} \rightarrow 10\ CO_2 + 2\ Mn^{2+} + 24\ H_2O$$

Procedure:

1) The original permanganate solution was diluted 1/20, boiled for 1hr, and allowed to stand overnight.
2) It was filtered through a fine-porosity sintered-glass funnel and stored in a brown bottle.
3) 0.120–0.150 gram samples of $Na_2C_2O_4$ (oven-dried for 1hr at 110 to 120°C) were transferred to 400ml beakers. Each sample of $Na_2C_2O_4$ was dissolved in 250ml of 0.9F H_2SO_4 and heated to 80–90°C.
4) The samples were titrated slowly with $KMnO_4$, using a thermometer as a stirring rod and maintained at a temperature >60°C.
5) 0.9F H_2SO_4 equal to the total volume at the endpoint.
6) From the corrected titration volume and the weight of $Na_2C_2O_4$, the normality of the $KMnO_4$ was calculated.

The concentration of the $KMnO_4$ was also found spectroscopically. Standard solutions of 0.0002N, 0.0008N, and 0.0012N (made from a standardized solution of 0.1N $KMnO_4$) were run on the spectrometer at 522nm and the ordinates were recorded. The $KMnO_4$ solution of unknown concentration was diluted 1/1000 and compared to the standards.

(e) 0.1M Na_2 EDTA—100 grams of Na_2 EDTA were dissolved in 2L of deionized water
(f) 0.6M picolinic acid—73 grams of picolinic acid were dissolved in 1L of deionized water (uptake by the resins drives the dissociation reaction)
(g) 0.3M $FeSO_4$ $7H_2O$—88 grams of $FeSO_4$ $7H_2O$ were dissolved in 1L of deionized water

2.2.2 Apparatus

The apparatus used in the initial tests for monitoring the resin degradation is shown in Figure 2.1. This design allows the resins to be in close contact with each other, and it allows gas generation and temperature variations to be observed by virtue of the water column; either process will cause a shift in the position of the water level which can be measured by reading off the graduated tubing to which the tygon connecting tube is attached. A different type of apparatus was used later in the main tests described later in Section 2.3.

The pH meter used was a Corning pH meter 125. The oven used for drying resins was a Thelco GCA/Precision Scientific Model 17. The spectrophotometer used was a Perkin-Elmer Model 320.

2.2.3 Procedures, Tests, and Experiments

Initial preparation of the ion exchange resins used in these experiments included regeneration, moisture content determinations and chelating/decontamination reagent or metal ion loading. These processes are summarized in Figure 2.2. Details of each procedure follow.

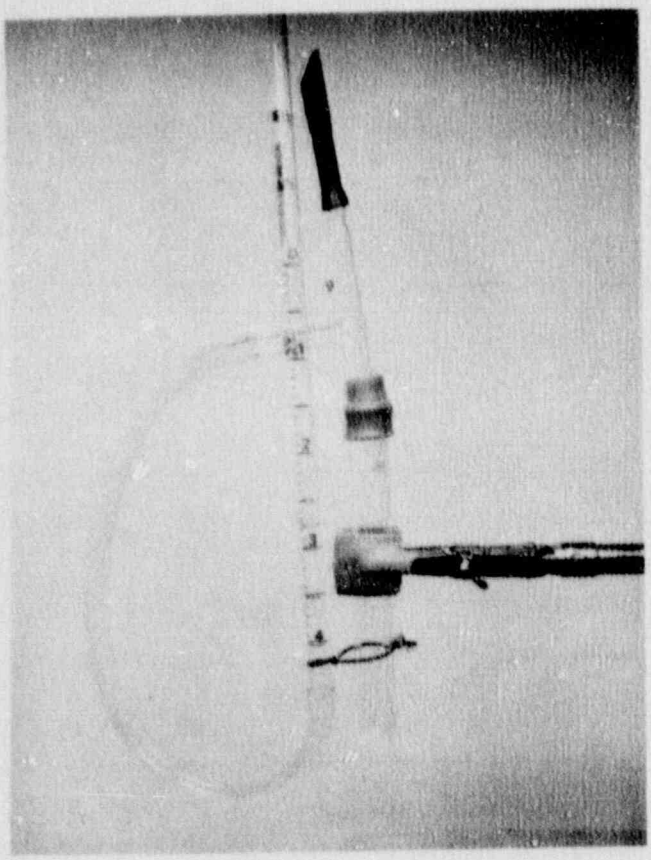

Figure 2.1 Apparatus for monitoring resin degradation.

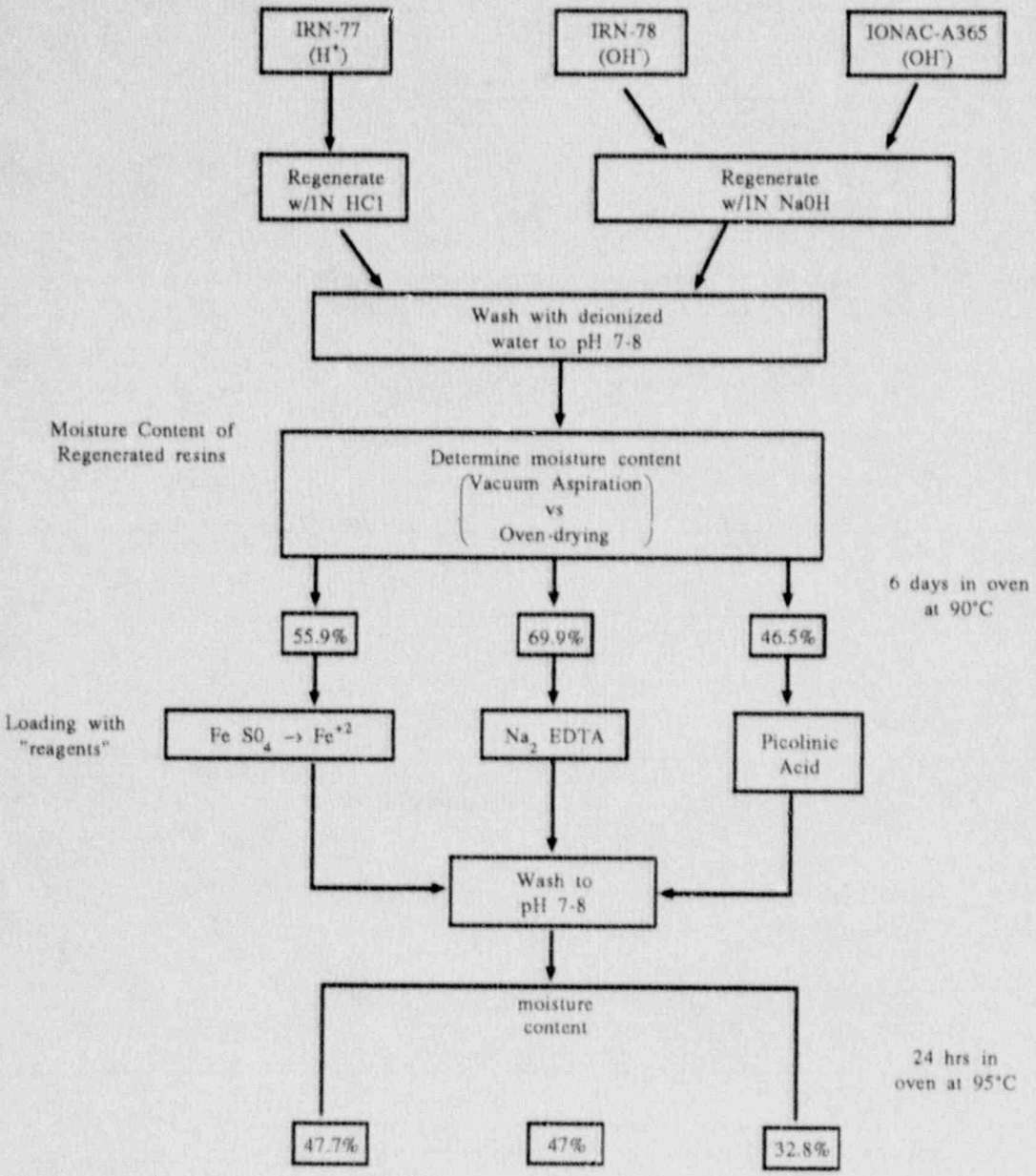

Figure 2.2 Flowchart of resin regeneration, moisture content determinations and EDTA, picolinic acid and Fe^{+2} loading.

2.2.3.1 Regeneration of Stock Resins

500 to 700 gram batches of stock IRN-77/H^+, IRN-78/OH^-, and IONAC A-365/OH^- were regenerated with 1N HCl, 1N NaOH, and 1N NaOH, respectively. Following regeneration, the resins were washed with deionized water until the pH of the rinse water was 7-8.

2.2.3.2 Determination of Moisture Content of Regenerated Resins

Each batch of resins was dewatered (vacuum-aspirated) for approximately 15 minutes and allowed to dry for approximately 15 minutes. Two samples were taken from each batch, weighed and oven-dried for 6 days at approximately 90°C. The difference in weight for vacuum-aspirated resins versus oven-dried resins was used to determine the moisture content of H^+ form of IRN-77 and the OH^- forms IRN-78, IONAC A-365.

2.2.3.3 Reagent Loading of Regenerated Resins

Batches of regenerated anion and cation resins were loaded with decontamination reagents and metal ions, respectively. The loading amounts were based on information provided by the resin manufacturer pertaining to exchange capacities (See Appendix A). IRN-77 resins were loaded with Fe^{+2}. The $FeSO_4$ solution was used to expend the resin batch based on two equivalents per mole of iron sulfate. 227 grams of resin were added to the solution, stirred, and allowed to stand for several days.

IRN-78 resins were loaded with disodium EDTA (Na_2 EDTA). The EDTA solution was assumed to provide one equivalent per mole. Then, 167 grams of resins were added to the solution, stirred, and allowed to stand for several days.

IONAC A-365 resins were loaded with picolinic acid. Sufficient picolinic acid was used to expend the resin batch based on one equivalent per mole. Next, 93 grams of resin were added to the solution, stirred, and allowed to stand for several days. Then, the resins were washed with deionized water until the pH of the resins was 7-8.

A sample from each batch was oven-dried for 24 hrs. at 95°C. Also, samples were vacuum-aspirated. The moisture contents were then determined in a manner similar to that for the "regenerated" resins. The results of these determinations are given in Figure 2.2.

2.2.3.4 Titrations with $KMnO_4$ and HNO_3

(a) Preliminary Determination of Regenerated Resin Sites Available Using MnO_4^-

A 5 gram sample of IONAC A-365 dewatered (vacuum-aspirated), regenerated resin was used for testing the approximate amount of MnO_4^- needed to place the resins in an "excess" oxidizing environment. This was done by adding MnO_4^- solution (13ml of 0.04N) dropwise until the pH of the supernatant became constant. This point was reached when the purple color of MnO_4^- persisted for several minutes. Then, the pH of the supernatant liquid over the resin was tested and the water volume was measured to allow a calculation of the amount of OH^- that had been released from the resins (presumably in exchange for MnO_4^-).

The results showed that approximatedly 2×10^{-6} moles of OH^- were present in the supernatant and that the amount of MnO_4^- used was approximately 5.2×10^{-4} moles. The amount of MnO_4^- taken up by the resins exceeded the "free" amount of OH^- calculated from the pH reading and the water volume. This implies that sites accepting MnO_4^- were not necessarily originally occupied by hydroxide ion.

(b) Exchange with $KMnO_4$ and HNO_3

Standard 5 gram samples of IONAC A-365 and IRN-78 resins were used to determine the pH change with the addition of incremental amounts of $KMnO_4$. Similar experiments to the one described above were performed with nitric acid. The resins were identically prepared, but 0.5M HNO_3 and 3M HNO_3, respectively, were added incrementally in each of the two experiments instead of $KMnO_4$.

(c) Determination of Equilibrium pH for IONAC A-365 and IRN-78 Resins in Water

Samples of the regenerated anion resins and the cation resin were taken and independently combined with deionized water to see if the pH corresponded with the starting pH (after regeneration, 7-8). The samples were allowed to equilibrate for two days and the pH was checked. The pH values were 9.17, 3.67, and 8.88 for IRN-78, IRN-77, and IONAC A-365, respectively. These values are all different from the 7-8 range reached after washing in the regeneration procedure. The alkaline pH of the anion resins indicates that they had liberated some hydroxide ion while the acidic pH of the cation resins indicates that hydrogen ions had been liberated.

(d) Determination of Fully Exchanged pH values for IONAC A-365 and IRN-78 with Nitric Acid

Five gram samples of dewatered (vacuum-aspirated) IONAC A-365 and IRN-78 were reacted with their calculated exchange capacity amounts of 3M HNO_3. They were allowed to equilibrate for approximately 20 minutes and the pH was checked. The amounts added were 16 and 7.3ml for IONAC A-365 and IRN-78 resin samples, respectively.

The low pH for the IONAC A-365 resins indicates that nitric acid above the exchange capacity for the resin was added. This may be linked to the differences in reporting of exchange capacities as meq/gm where the weight maybe "dry," "dewatered," etc. Apparently the "dry weight" exchange capacity for these resins is sufficiently higher than the exchange capacity per gram of "dewatered" or "vacuum-aspirated" weights used in the experiments to cause the excess acid observed.

For the IRN-78 resins, the nitrate-for-hydroxide ion exchange would appear to have taken place successfully, but the neutralization of released hydroxide by the hydrogen ions from nitric acid did not occur to a sufficient extent to bring the pH down from the basic range. It is not clear what would cause this situation.

2.2.4 Results and Discussion

2.2.4.1 Moisture Content Determinations

The determination of the moisture content of dewatered resins makes it possible to specify consistent resin amounts based on weight, i.e., the moisture content allows one to take into account any water that may remain attached to the resins.

The moisture content of the regenerated resins (hydroxide and hydrogen ion forms for anion and cation resins, respectively) and the "loaded" resins was taken as the difference in weight between the dewatered (vacuum-aspirated) state and the oven-dried state. Table 2.2 shows the results of this determination for the regenerated resins. The average moisture content for IRN-78/OH^- resins, was 69.9%, for IRN-77/H, 55.9%, and for IONAC A-365/ OH^- resins, 46.5%.

Table 2.3 gives the results of the moisture content determination for the "loaded" resin batches. The average moisture content for IRN-78 resins loaded with EDTA was 47.0%; for IRN-77 resins loaded with Fe^{+2}, 47.7%, and for IONAC A-365 resins loaded with picolinic acid, 32.8%.

A comparison of Tables 2.2 and 2.3 shows that, for IRN-77, the moisture content of the H^+ form is ~8% higher than that for the Fe^{+2} loaded form. The +2 charge on the iron means that only one-half as many ions (Fe^{+2}) may occupy the fixed ionic sites of the resin as compared to the +1 charge on the hydrogen ion. This may lead to a decrease in associated "hydration" moisture attached to the Fe^{+2} versus that attached to H^+.

The anion resin, IRN-78 exhibited a moisture content of 69.9% for the OH^- form versus 47% for the EDTA form. The EDTA molecule is considerably larger than the hydroxide ion. It is also capable of existing in a number of ionic states, +2 to −4, depending on the pH. Near neutral pH, the principal forms of EDTA are the −2 and −3 states. Compared to hydroxide ion (−1), two or three times as many fixed ion sites could be

Table 2.2

Results of moisture content determinations for regenerated resins (OH^- and H^+ forms)

Resin Type	Mass of Vacuum Aspirated Sample (g)	Mass of Sample After Oven-Drying (g)	Moisture Content Mass %
1) IRN-78	7.6	2.3	69.5
2) IRN-78	7.9	2.4	69.7
3) IONAC A-365	7.5	4.0	46.5
4) IONAC A-365	10.1	5.4	46.5
5) IRN-77	11.4	5.0	56.2
6) IRN-77	11.9	5.3	55.7

Table 2.3

Results of moisture content determinations for "reagent-loaded" resins

Resin Type (Reagent-Loaded)	Mass of Vacuum Aspirated Sample (g)	Mass of Sample After Oven Drying (g)	Moisture Content Mass %
1) IONAC A-365 (Loaded with PA)[a]	6.84	4.60	32.8
2) IONAC A-365 (PA)	5.40	3.63	32.8
3) IRN-78[b] (EDTA)[c]	6.44	3.42	46.9
4) IRN-78 (EDTA)	6.56	3.47	47.1
5) IRN-77 (Fe^{+2})	4.40	2.31	47.5
6) IRN-77 (Fe^{+2})	5.50	2.86	48.0

[a] PA = picolinic acid.
[b] IRN-78 = the IRN-78 resin results are subject to consideration of nitrogen functionality loss on oven drying (see Appendix A).
[c] EDTA = ethylenediaminetetraacetic acid.

occupied by EDTA as by hydroxide ion. There would thus be expected to be less associated "hydration" water with a lower net counter ion population.

Similar results occurred for the IONAC A-365 resins loaded with picolinic acid. The picolinic acid group is expected to have a −1 charge identical to hydroxide ion, however, it is a much larger molecule and may therefore allow accommodation of less associated water in the resin structure than hydroxide ion.

2.2.4.2 Anion Resin Titrations with HNO_3 and $KMnO_4$

IRN-78 and IONAC A-365 anion resins were titrated with nitric acid. The resins were originally in the OH^- form. When nitric acid was added, they exchanged their OH^- ions for NO_3^- ions. The OH^- ions liberated were neutralized by the H^+ from the nitric acid. These reactions may be described by the following three equations:

$$HNO_{3\,(aq)} \longleftrightarrow H_{(aq)} + NO^-_{3\,(aq)} \qquad (1)$$

$$OH^-_{(resin)} + NO^-_{3\,(aq)} \longleftrightarrow NO^-_{3\,(resin)} + OH^-_{(aq)} \qquad (2)$$

$$OH^-_{(aq)} + H^+_{(aq)} \longleftrightarrow H_2O \qquad (3)$$

IRN-78 resins titrated with 0.5M and 3M HNO_3 (Figure 2.3) behaved similarly to a typical titration of a strong acid resin. The IRN-78 resins readily gave up their OH^- ions for

NO_3^- ions. When all of the OH^- ions had been replaced by NO_3^- ions, the pH decreased sharply with further addition of nitric acid.

The exchange capacity of the IRN-78 resin was determined at neutral pH and found to be 4.7 meq/gm (vacuum-aspirated, OH^- form). This value differs by about 0.4 units compared to the exchange capacity reported by Rohm and Haas, 4.3 meq/gm dry weight (see Appendix A).

IONAC A-365 and IRN-78 titrated with 3M HNO_3 produced the titration curves given in Figure 2.4. These are similar in shape but different in relative position. The NO_3^- ions were taken up by both the IRN-78 and the IONAC A-365 resins, while the OH^- ions were being released. At the same time, the OH^- ions were being neutralized by the H^+ ion of the nitric acid, thus decreasing the pH of both resins.

The shift of the titration curve of the IRN-78 resin to the right indicates that the IRN-78 resins are capable of taking on nitrate ion more readily than the IONAC A-365 resins. The initial pH of the IRN-78 resins was 13. This would indicate that the IRN-78 resins are very willing to give up their OH^- ions. Compared to the IRN-78, the IONAC A-365 resins did not readily release OH^- ions; the IONAC A-365 initial pH was about 9.

The exchange capacities of IONAC A-365 and IRN-78 were determined at neutral pH and found to be 3.8 meq/gm and 6.5 meq/gm (vacuum-aspirated, OH^- form) for IONAC A-365 and IRN-78, respectively.

Table 2.4 gives a comparison of the experimental and literature exchange capacities.

The IONAC A-365 resin moisture content (for the OH^- form) was found to be 46.5%. This would lead to a low exchange capacity for vacuum-aspirated samples compared to dry weight samples. IRN-78 resins remained at high pH for extended periods (>pH 12). Sorption phenomena are enhanced on these types of resins under these conditions (Moody and Thomas, 1972); it is thought that a significant fraction of the nitrate ion was sorbed as well as exchanged with the fixed ionic groups of the resin.

A preliminary study in which 2 ml increments of 0.5M nitric acid were added to IONAC A-365 resins in OH^- form was performed. With each acid addition, the pH was monitored for 40 minutes. The sample was thoroughly stirred. The resins showed a slow, continuous increase in pH upon each acid addition. These results indicated that equilibrium was not quickly attained; the IONAC A-365 resins exchange OH^- for NO_3^- very slowly.

Following this, another experiment was performed with the results shown in Figure 2.5. The titration of IONAC A-365 with 0.5M HNO_3 not only looked at the pH change with each addition of nitric acid, but also the effect of time on the pH. The pH was monitored 5 minutes and 10 minutes after each acid addition. The titration curve showed that the pH of the IONAC A-365 resin five minutes after acid addition varied little within the next five minutes. Both of these studies show that even though the resins readily exchanged ions, the exchange proceeded at a slow rate.

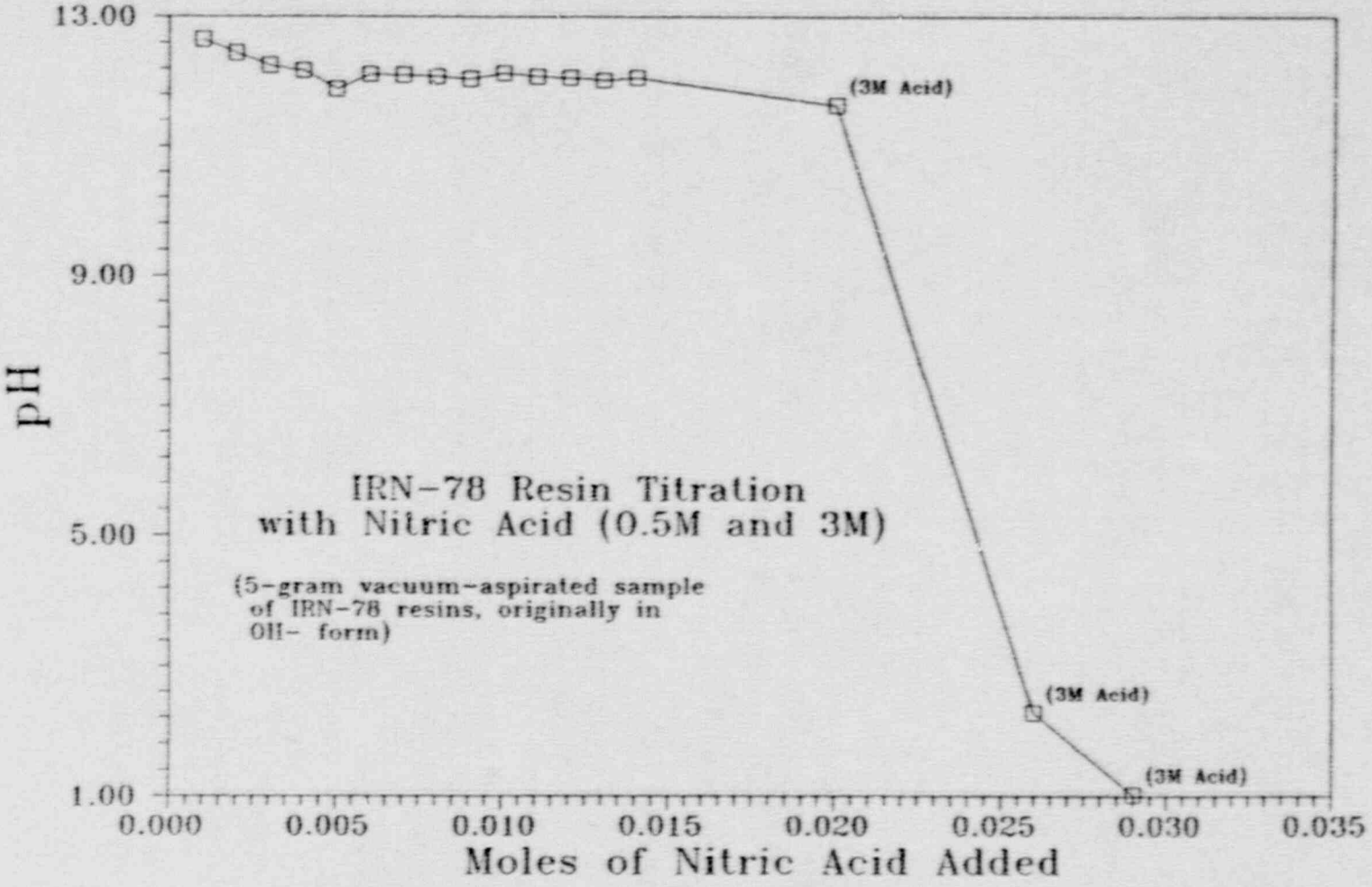

Figure 2.3 IRN-78 resin titration with nitric acid.

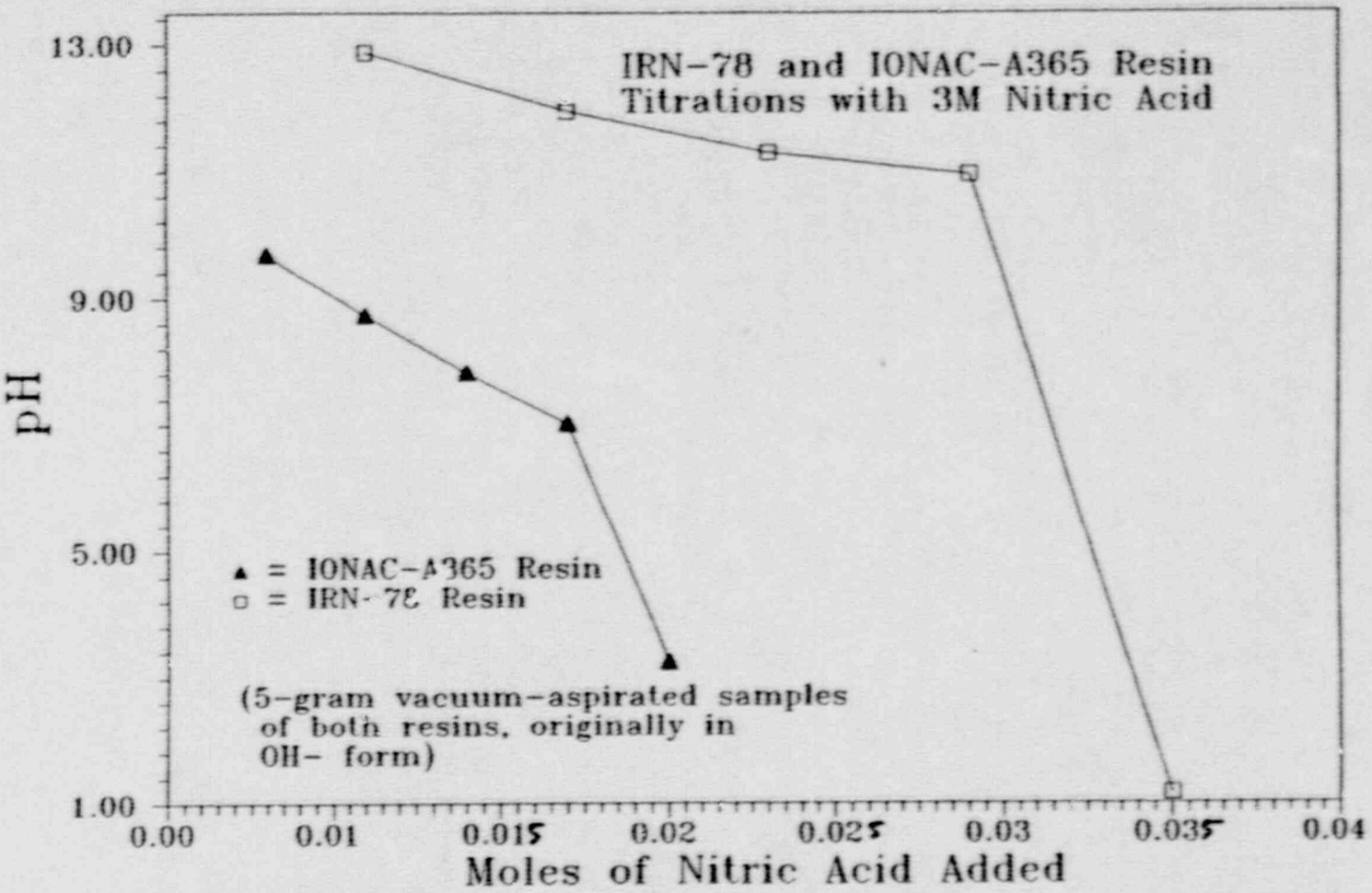

Figure 2.4 IRN-78 and IONAC A-365 resin titrations with nitric acid.

Table 2.4

Exchange capacities for IONAC A-365 and IRN-78 resins

	Experimental	Literature[a]
IONAC A-365 (OH^-)	3.76 meq / gm (vacuum-aspirated)	9.5 meq / gm (dry weight)
IRN-78 (OH^-)	6.50 meq / gm (vacuum-aspirated)	4.3 meq / gm (dry weight)

[a]Appendix A.

The titration curve in Figure 2.5 also showed certain points at which the pH dropped very sharply. In the first case (at 16 ml of acid added), the pH decreased slightly, but ten minutes after acid addition, it had risen to a point coinciding with the general trend of the curve. In the next case, the pH dropped to about 3.9 (at 22 ml of acid added). Ten minutes after acid addition, the pH still remained at 3.9. Upon the next addition of nitric acid, the pH rose to 7.0. The exact cause(s) of the sudden drop in pH is unknown. An effort was made to keep the resins stirred so that no local pockets of acid would develop. The fact that on the next acid addition the pH rose to a point coinciding with the general trend of the curve indicates no obvious flaw in the experimental procedure.

IRN-78 and IONAC A-365 resins were also titrated with 0.04N potassium permanganate (initial pH of the permanganate solution was 6.6). The results of this experiment are given in Figure 2.6. The resins were originally in the OH^- form. When permanganate ions were added, the resins exchanged their OH^- ions for MnO_4^- ions. The characteristic purple color of permanganate disappeared as the resins exchanged OH^- for MnO_4^-. When the purple color of MnO_4^- persisted for several minutes, it was assumed that the maximum amount of permanganate had been taken up by the resins and thus, the permanganate remained in the supernatant layer. The liberated hydroxide ions were not neutralized in this titration. As a result, the pH of both the IRN-78 and IONAC A-365 resins increased. These reactions may be described by the following expressions:

$$KMnO_4 \longleftrightarrow K^+_{(aq)} + MnO^-_{4\,(aq)} \qquad (4)$$

$$OH^-_{(resin)} + MnO^-_{4\,(aq)} \longleftrightarrow OH^-_{(aq)} + MnO^-_{4\,(resin)} \qquad (5)$$

As the titration proceeded, the resins reached an almost steady equilibrium state, i.e., no further changes in pH were observed with further addition of permanganate ion.

2.2.4.3 Reactions of IRN-78 and IONAC A-365 Resins with $KMnO_4$ and HNO_3

Individual 5 gram samples of oven-dried, regenerated IONAC A-365 and IRN-78 resins were placed in the monitoring apparatus (Figure 2.2). To each was added 5 ml of 0.04N $KMnO_4$ in bulk. Both samples produced a small amount of heat; there was a clear

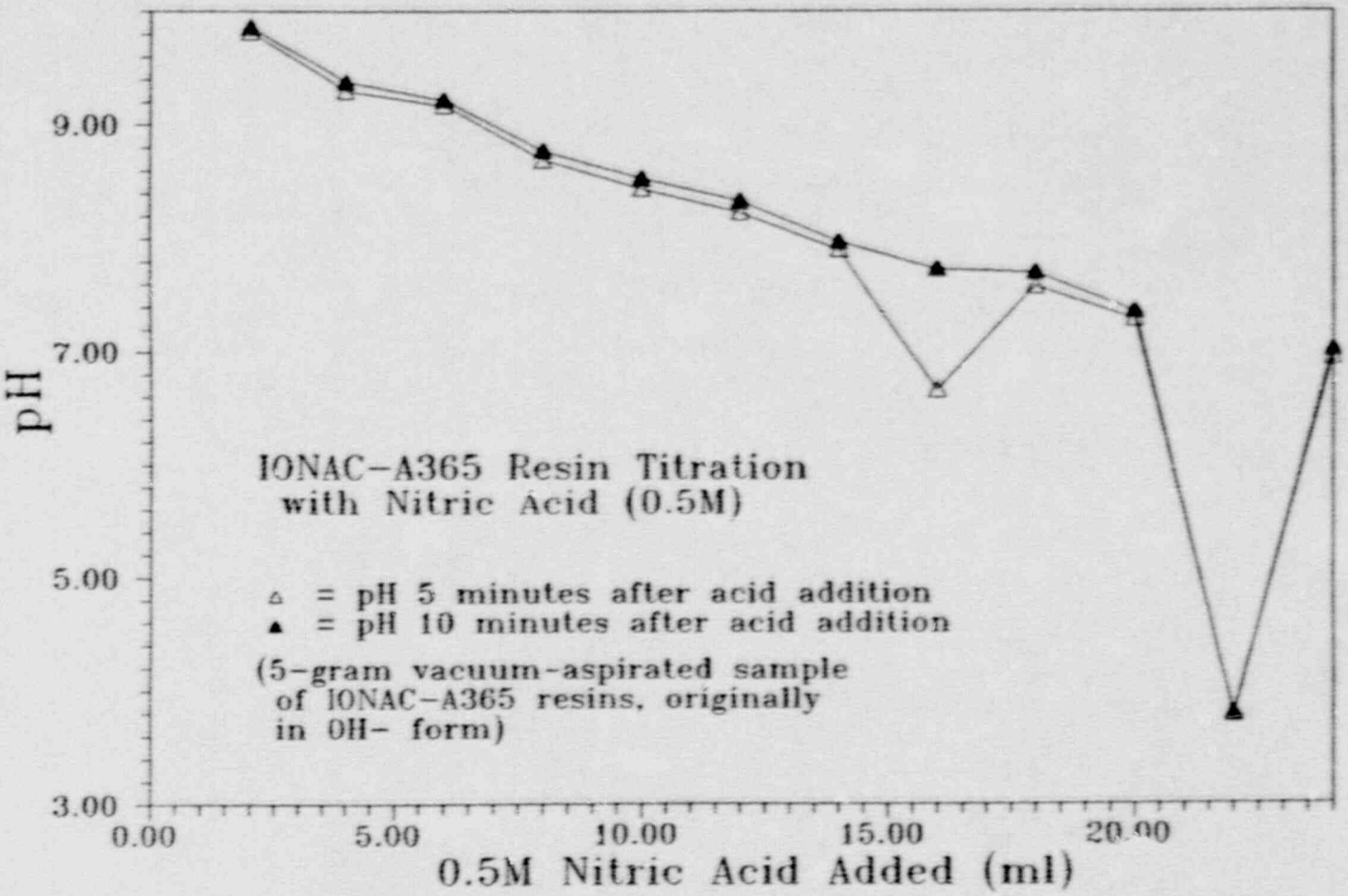

Figure 2.5 IONAC A-365 resin titration with nitric acid—time study.

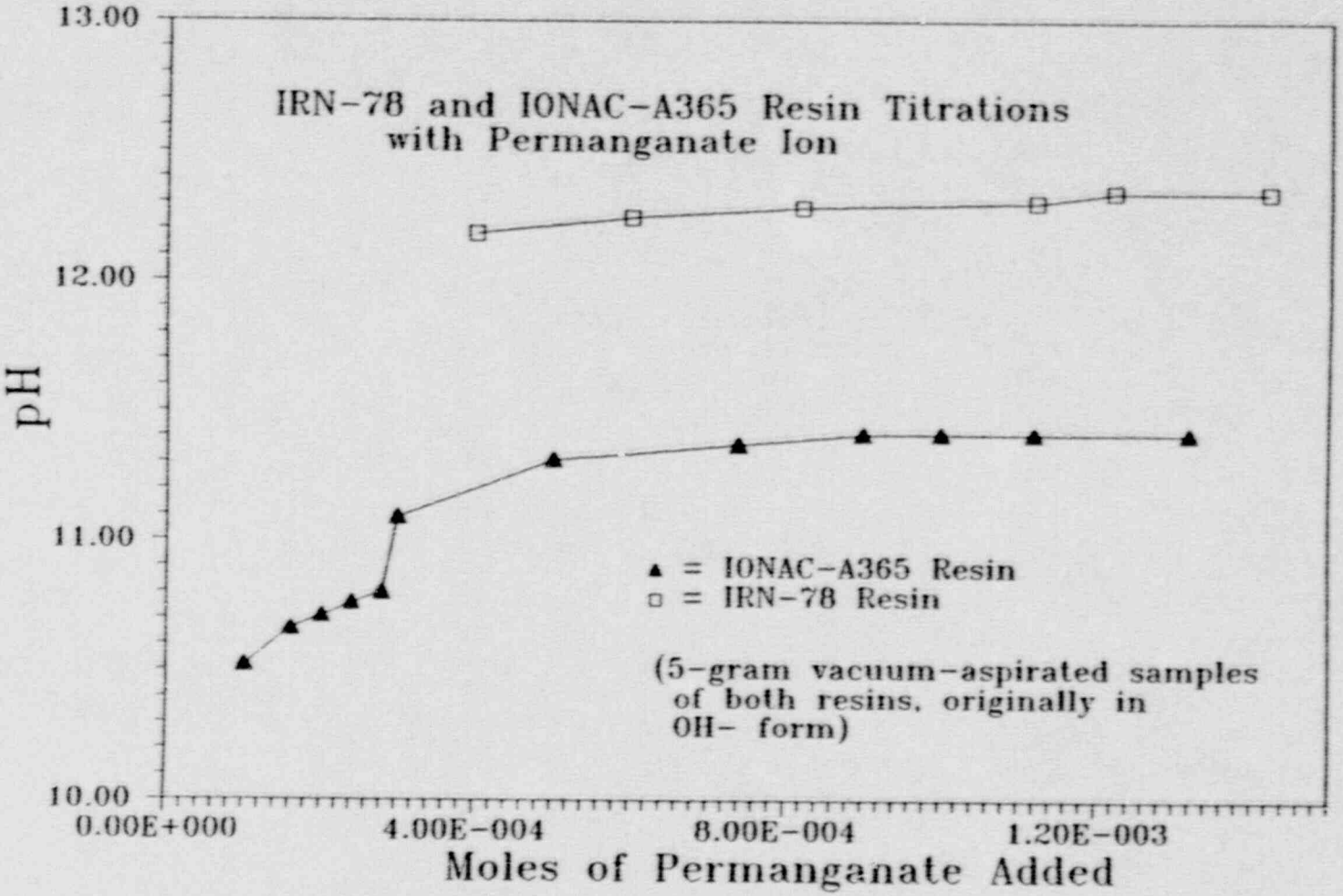

Figure 2.6 IRN-78 and IONAC A-365 resin titrations with permanganate ion.

supernatant layer as well as black MnO_2 present. In addition, the IONAC A-365 resin beads at the top experienced some swelling.

This test was repeated with 4ml and 6.4ml of 3M HNO_3 for oven-dried samples of IONAC A-365 and IRN-78, respectively. The IONAC A-365 gave off a steam-like gas, the resin beads at the top swelled, and, after the reaction, the water level in the monitoring apparatus dropped suddenly. The IRN-78 resin sample started to bubble and foam immediately upon the addition of the nitric acid. During this time, slight smoke was given off. The water level in the monitoring apparatus oscillated before it rose to an intermediate level at which it remained for a few hours. At the end of the day, the level had gradually fallen.

Next, 1 gram samples of dewatered (vacuum-aspirated) IONAC A-365 and IRN-78 were placed in the monitoring apparatus and subjected to nitric acid. 5ml and 2ml of HNO_3 were added dropwise to IONAC A-365 and IRN-78, respectively. The samples experienced no reaction, but the IRN-78 resins experienced a distinct color change from brown to yellow.

This experiment was repeated with oven-dried samples to determine the effect of the dewatering on the reactions. One gram oven-dried samples of IONAC A-365 and IRN-78 were subjected to nitric acid. Increments of 3ml and 4ml of 3M HNO_3 were added dropwise to IONAC A-365 and IRN-78, respectively. The IONAC A-365 resin sample produced a small amount of heat. The IRN-78 resin sample gave off traces of smoke with each addition of nitric acid. These results are summarized in Figure 2.7.

A comparison of the reaction results for oven-dried resins versus dewatered (vacuum-aspirated) resins upon nitric acid addition shows that the drying of the resin has an effect on the extent of the reaction of the resins with HNO_3.

A comparison of the reaction results for dropwise addition of nitric acid versus bulk addition of nitric acid shows that the way in which the nitric acid is added also has a strong bearing on the extent of the reaction.

Resins treated with potassium permanganate reacted to a lesser extent than those treated with nitric acid. Both chemicals are oxidizing agents but a comparison of their relative oxidizing "strength" is not appropriate since the concentrations varied by nearly two orders of magnitude, i.e., the nitric acid was much more concentrated than the permanganate.

2.2.5 Conclusions for Preliminary Experiments

a) IRN-78, IONAC A-365 and IRN-77 organic ion exchange resin moisture contents vary significantly depending on the counter ion "loading." For these resins the EDTA, picolinic acid and Fe^{+2} "loaded" forms, respectively, had moisture contents lower than the regenerated, OH^- and H^+ "loaded" forms.

Reactons with $KMnO_4$ and HNO_3

IONAC-A365/OH^- (oven-dried)	+	0.04M $KMnO_4$ (bulk)	Small amount of heat, water layer and black MnO_2 present, upper beads swelled.
IRN-78/OH^- (oven-dried)	+	0.04M $KMnO_4$ (bulk)	Small amount of heat water layter and black MnO_2 present
IONAC-A365/OH^- (oven-dried)	+	3M HNO_3 (bulk)	Steam-like gas, upper beads swelled
IRN-78/OH^- (oven-dried)	+	3M HNO_3 (bulk)	bubbled and foamed, slight smoke
IONAC-A365/OH^- (dewatered)	+	3M HNO_3 (dropwise)	No reaction
IRN-78/OH^- (dewatered)	+	3M HNO_3 (dropwise)	Distinct color change (brownish - yellow)
IONAC-A365/OH^- (oven-dried)	+	3M HNO_3 (dropwise)	Small amount of heat
IRN-78/OH^- (oven-dried)	+	3M HNO_3 (dropwise)	Traces of smoke

Figure 2.7 Summary of reactions of resins with potassium permanganate and nitric acid solutions.

b) In determinations of resin exchange capacities, care must be taken that conditions are such that equilibrium can be reached (i.e., sufficient time is allowed for the resins to exchange with the solution) and that sorption effects are minimized. In reporting exchange capacities, information must be provided about the specific condition of the resins tested, e.g., meq per gram of oven-dried, original OH^- form resin.

c) Heat- and gas- generating reactions have been observed with the two anion resins used, IRN-78 and IONAC A-365. The resins were originally in the OH^- form and potassium permanganate (0.04M) and nitric acid (3M) were oxidizing solutions used to produce the reactions. The extent/vigor of the reaction is very highly dependent on the degree of dewatering of the resins and (probably linked to this) on the method of solution addition (dropwise or in bulk). The heat generation may be due, in part, to the heat of neutralization (acid addition to hydroxide-form resins). Further observations included that the IRN-78 resins underwent a color change upon addition of nitric acid and the IONAC A-365 resins exhibited noticeable swelling in both the potassium permanganate and nitric acid experiments.

2.3 Primary Experiments

The main experiments on resin degradation were based on the preliminary tests described in Section 2.2. However, the equipment was redesigned in order to obtain more comprehensive information.

2.3.1 Apparatus and Procedures

Figure 2.8 shows the new apparatus for studying the effects of nitric acid/potassium permanganate additions to simulated resin waste. It consists of a Buchner funnel in which the resins are placed in readiness for reaction with nitric acid alone or nitric acid followed by potassium permanganate. The base of the funnel has a porous frit on which the resin is placed. A rotary vacuum pump is used to aspirate the wet starting resins or to remove reagents that have reacted with them for further study.

The anion and cation resins used in the study were in the as-received conditions and were loaded with picolinic acid, EDTA, or Fe^{+2} using a simple batch process. In this, 200g batches of resin were stirred into 2L of deionized water containing amounts of picolinic acid, EDTA, or $FeSO_4$ to give either 50 or 100 percent theoretical loading of the resin.

In the resin/reagent interaction experiments, the resins were either in an "oven-dried" or vacuum aspirated condition. Oven dried experiments were carried out on 5 g quantities of resin placed in the Buchner funnel or on 5 or 10 g quantities of the aspirated material which remained in a heavier water-swollen condition.

Chemically-induced thermal excursions were studied by adding 3M HNO_3 to the loaded resins in the Buchner funnel in dropwise or bulk increments. For the dropwise tests, 50 drops of the acid were allowed to fall on the resins which was sufficient to "saturate" the resin mass. At this point, visual observations were made to check for smoke or increases in

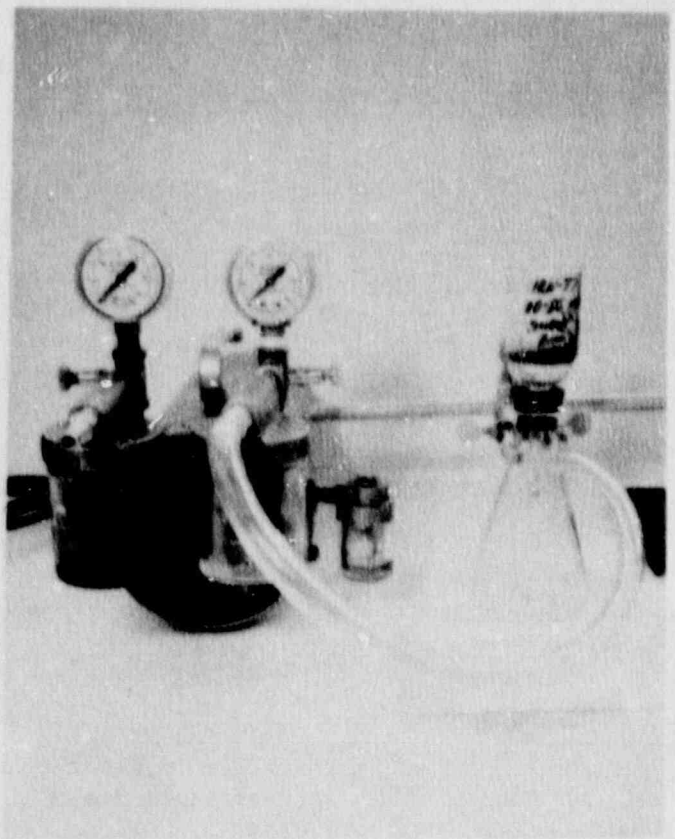

Figure 2.8 Apparatus for studying reactions between ion-exchange resins and decontamination reagents.

temperature. Two additional 50 drop increments of acid were subsequently administered and observations made after each step. In total, the 150 drops of HNO_3 amounted to a volume of 7 mL.

In tests where ~0.8N $KMnO_4$ was added after the nitric acid additions, the reagents was added in three 3 mL increments. Changes in color or temperature of the resin/reagent mixture were monitored after each addition. Any temperature changes caused by air-oxidation reactions were followed using a thermocouple immersed in the resins. In some instances, precipitates were formed on the stem of the Buchner funnel. These occurred almost immediately in some cases, and days later in others after water evaporation had occurred.

In some of the final experiments, reagent additions were made in 100 mL increments in order to quickly saturate the resins and to determine if larger changes in reaction rates could be induced. This would enhance the chances of determining which reactions were of greater significance with respect to heat up scenarios.

2.3.2 Results and Discussion

The results of the HNO_3 / $KMnO_4$ additions are discussed for both oven-dried and vacuum aspirated (dewatered) resin mixtures which had been fully or partly loaded with picolinic acid, EDTA, or $FeSO_4$. Values of the pH for the resins and eluates after reaction were measured and color changes, and vapor/smoke generation were noted when present. Any changes in temperature were measured since this would be one of the most likely indications of chemical change.

Table 2.5 shows that for over-dried IRN-78 and IONAC A-365 anion resins loaded with picolinic acid the addition of 3M HNO_3 , in drop or bulk form, caused a rise in the resin temperature. Increases of up to 15°C were detected. The pH of the resin moisture and the eluate were often lowered to values less than 1.0. White precipitates formed on the stem of the Buchner funnel with time and samples were removed for examination. Usually, bulk additions of HNO_3 caused smoke generation and bubbles, indicating gas generation. The dropwise addition of HNO_3 usually did not cause smoke to form. When $KMnO_4$ was added, at a time long after the HNO_3 reaction had ceased (usually after a few days), no change was noted in the resin temperature. However, the pH of the resins and eluates showed some increase. During vacuum aspiration some vapor production was observed in the filtering flask. This was occasionally accompanied by a cooling of the filteration flask indicating that the vapor was composed of a frozen aerosol of reagent. This would form as a result of high velocity air passing through the resin during vacuum aspiration.

For oven-dried resins loaded with EDTA similar increases in temperature were noted for HNO_3 additions. No significant changes in temperature were noted when $KMnO_4$ was later added to the various resin / HNO_3 systems. As was the case for the picolinic acid loaded resins the EDTA / resin mixtures often showed vapor production in the filtering flask during aspiration. Smoke production, however, was not common.

Table 2.5 Chemical interactions between nitric acid/potassium permanganate combinations and oven-dried anion exchange resins loaded with decontamination reagents.

Resin Type, Organic Acid & Percent Loading	Added Chemical & Method of Addition: bulk (b) or drops (d)	Vacuum Aspiration Performed Following:	Initial Resin Bed Temperature (°C)	Maximum Resin Bed/Slurry Temp. Measured (°C)	pH		Color				General Observations
					Resin Bed Slurry	Eluate	Initial Resin Bed Slurry	Final Resin Bed Slurry	Final Eluate	Precipitate Color	
IRN-78-50%-PA	3MHNO_3:d	150 drops (~7ml)	25	31	1.29	1.17	Orange/Amber	Lighter-Orange/ Amber	Light Yellow Tint	White	Some signs of smoke with 1st 50 drops of 3M HNO_3 only.
IRN-78-100%-PA	3MHNO_3:d	150 drops (~7ml)	25	40	1.19	1.31	Medium Amber	Medium Amber	Moderate Yellow Tint	White	No visible reactions observed; i.e., no smoke etc.
IONAC A-365-50%-PA	3MHNO_3:d	150 drops (~7ml)	25	35	2.34	1.59	Yellow/White	Light Brown	Clear	White	No visible reactions.
IONAC A-365-100%-PA	3MHNO_3:d	150 drops (~7ml)	26	35	1.58	1.36	Off White	Light Brown	Clear	White	No visible reactions.
IRN-78-50%-PA	3MHNO_3:b	9ml	26	37	0.57	0.66	Orange Amber	Light Orange/ Amber	Light Yellow Tint	White	Smoke generation and bubbling in resin bed.
IRN-78-100%-PA	3MHNO_3:b	9ml	26	36	0.62	0.72	Medium Amber	Light Orange/ Amber	Med. Yellow Tint	White	Some bubble generation; no other reactions observed.
IONAC A-365-50%-PA	3MHNO_3:b	9ml	30	38	1.02	1.05	Yellow/White	Med. Yellow/ White	Slight Yellow Tint	White	Some minor bubbling and temperature rise.
IONAC A-365-100%-PA	3MHNO_3:b	9ml	28	34	0.67	0.71	Off White	Light Brown	Slight Yellow Tint	White	Same as above.
IRN-78-50%-PA	3MHNO_3/KMnO_4:d	150 drops	28	-	-	1.40	Light Orange/ Amber	Light Orange/ Amber	Brownish-Green	White	Vapor cloud production in filtering flask during vacuum aspiration. No reactions observed.
IRN-78-100%-PA	3MHNO_3/KMnO_4:d	150 drops	28	30	-	1.81	Medium Amber	Medium Amber	Slight Yellow Tint	White	Vapor cloud production during vacuum aspiration.
IONAC A-365-50%-PA	3MHNO_3/KMnO_4:d	150 drops	29	29	3.84	3.60	Light Brown	Light Brown	Slight Brown	White	No vapor cloud production during vacuum aspiration.
IONAC A-365-100%-PA	3MHNO_3/KMnO_4:d	150 drops	30	30	3.65	-	Light Brown	Light Brown	Clear	White	Vapor cloud production during vacuum aspiration.
IRN-78-50%-PA	3MHNO_3/KMnO_4:b	9ml	30	30	-	1.19	Light Orange/ Amber	Light Orange/ Amber	Brownish-Green	White	Vapor cloud production during vacuum aspiration.
IRN-78-100%-PA	3MHNO_3/KMnO_4:b	9ml	31	30	1.12	1.17	Light Orange/ Amber	Light Orange/ Amber	Brownish-Green	White	Vapor cloud production during vacuum aspiration, bottom of flask quite cool.
IONAC A-365-50%-PA	3MHNO_3/KMnO_4:b	9ml	30	30	3.06	-	Med. Yellow/ White	Med. Yellow/ White	Clear	White	Vapor cloud production during vacuum aspiration, filtering flask cool.
IONAC A-365-100%-PA	3MHNO_3/KMnO_4:b	9ml	30	31	3.30	2.17	Light Brown	Light Brown	Amber	White	Vapor cloud production during vacuum aspiration, no temperature decrease on bottom of flask.
IRN-78-100%-EDTA	3MHNO_3:d	Each 100 drop addition	22	32	-	0.40	Orange/Amber	Lighter Amber	Yellowish	None	Vapor cloud production during vacuum aspiration.
IRN-78-100%-EDTA	3MHNO_3:b	Each 5ml addition	21	29	-	0.20	Orange/Amber	Lighter Amber	Yellowish	None	No vapor production; initial drops produced smoke, temperature increases with stirring.
IONAC A-365-100%-EDTA	3MHNO_3:d	Each 50 drop addition	20	28	-	0.06	Cream/Yellow	Cream/Yellow	Clear	None	Vapor cloud production during vacuum aspiration.

Table 2.5 Chemical interactions between nitric acid/potassium permanganate combinations and oven-dried anion exchange resins loaded with decontamination reagents. (Cont'd)

Resin Type, Organic Acid & Percent Loading	Added Chemical & Method of Addition: bulk (b) or drops (d)	Vacuum Aspiration Performed Following:	Initial Resin Bed Temperature (°C)	Maximum Resin Bed/Slurry Temp. Measured (°C)	pH		Color				General Observations
					Resin Bed Slurry	Eluate	Initial Resin Bed Slurry	Final Resin Bed Slurry	Final Eluate	Precipitate Color	
IONAC A-365-100%-EDTA	$3MHNO_3$;b	Each 5ml addition	21	29	-	0.23	Cream/Yellow	Cream/Yellow	Clear	None	Vapor cloud production during vacuum aspiration.
IRN-78-100%-EDTA	$3MHNO_3$;$KMnO_4$;d	Each 75 drop addition	20	29	-	0.42	Orange/Amber	Orange/Amber	Clear	None	Vapor cloud production during vacuum aspiration.
IRN-78-100%-EDTA	$3MHNO_3$;$KMnO_4$;b	Each 5ml addition	21	21	-	0.55	Orange/Amber	Orange/Amber	Clear	None	Vapor cloud production during vacuum aspiration.
IONAC A-365-100%-EDTA	$3MHNO_3$;$KMnO_4$;d	Each 100 drop addition	21	21	-	2.79	Cream/Yellow	Maroon	Clear	Slightly white	Vapor cloud production during vacuum aspiration.
IONAC A-365-100%-EDTA	$3MHNO_3$;$KMnO_4$;b	Each 5ml addition	22	23	-	1.32	Cream/Yellow	Light Brown	Clear	White	Vapor cloud production during vacuum aspiration.

Table 2.6 shows similar tests on dewatered resins. Compared to the oven-dried resins, the addition of HNO_3 caused only a modest temperature increase for anion resins loaded with picolinic acid. Resins loaded with EDTA showed similar small temperature increases when HNO_3 was added. When $KMnO_4$ was subsequently added to the acidified resins, again no temperature increases were noted. During the addition of HNO_3 and $KMnO_4$ smoke was not observed but vapor was often seen in the filtering flask during aspiration.

The results of HNO_3 / $KMnO_4$ additions to cation resins loaded to their full ion-exchange capacity with ferrous ion are summarized in Table 2.7. Similarities to the anion results are clearly evident with temperature increases noted only for HNO_3 additions to oven-dried resins. Subsequent additions of $KMnO_4$ did not lead to temperature increases. No temperature changes were seen for aspirated resins when HNO_3 and $KMnO_4$ were added in sequence. Also, no precipitation was ever found for cation resin experiments. The pH values for the eluates were usually zero after HNO_3 additions but rose slightly after $KMnO_4$ was added. Vapor formation was not noticed in the cation resin tests.

In summary, it seems that heat is generated only when HNO_3 is added to anion or cation resins in the oven-dried condition. The magnitude of the increase does not sensitivity depend on whether the resins are of the anion or cation form, or on the ionic specie loaded on them. Most probably, the heat is released because of a resin hydration reaction. Additions of $KMnO_4$ to the resins which have been hydrated by the HNO_3 solutions do not cause any additional temperature change. At this time, the limited studies performed to date do not show any abnormal behavior that could be linked to thermal excursions that were occasionally experienced in industry. It would appear that such excursions can only be induced by some rare combination of waste composition, contamination, and dewatering process which still remains unkwown.

Work on this particular task is now being terminated, with only a few simple tests being planned to check the chemical nature of the precipitates that were formed from the resin / reagent interactions.

Table 2.4 Chemical interactions between nitric acid/potassium permanganate combinations and vacuum-aspirated anion exchange resins loaded with decontamination reagents.

Resin Type, Organic Acid & Percent Loading	Added Chemical & Method of Addition: bulk (b) or drops (d)	Vacuum Aspiration Performed Following:	Initial Resin Bed Temperature (°C)	Maximum Resin Bed/Slurry Temp. Measured (°C)	pH		Color				General Observations
					Resin Bed Slurry	Eluate	Initial Resin Bed Slurry	Final Resin Bed Slurry	Final Eluate	Precipitate Color	
IRN-78-50%-PA	1MHNO_3:d	Each 50 drop addition	26	33	-	0.61	Amber	Pale Amber	Clear	None	Vapor cloud production during vacuum aspiration. Bubbles seen under filter frit.
IRN-78-100%-PA	1MHNO_3:d	Each 50 drop addition	26	29	-	0.52	Orange/Amber	Light Yellow/ Amber	Clear	None	Vapor cloud production during vacuum aspiration. Bubbles seen under filter frit.
IONAC A-365-50%-PA	1MHNO_3:d	Each 50 drop addition	24	29	-	0.56	Yellow/White	Yellow/White	Clear	White	Vapor cloud production during vacuum aspiration.
IONAC A-365-100%-PA	1MHNO_3:d	Each 50 drop addition	24	28	-	0.61	Yellow/Tan	Yellow/Tan	Clear	White	Vapor cloud production during vacuum aspiration.
IRN-78-50%-PA	1MHNO_3:b	Each 5ml Addition	24	30	-	0.71	Amber	Light Yellow/ Amber	Clear	White	Vapor cloud production during vacuum aspiration.
IRN-78-100%-PA	1MHNO_3:b	Each 5ml Addition	25	28	-	0.54	Orange/Amber	Yellow/Amber	Clear	None	Some vapor production during vacuum aspiration. bubbles beneath filter frit.
IONAC A-365-50%-PA	1MHNO_3:b	Each 5ml Addition	24	29	-	0.55	Yellow/White	Yellow/White	Clear	White	No vapor production.
IONAC A-365-100%-PA	1MHNO_3:b	Each 5ml Addition	24	29	-	0.60	Yellow/Tan	Yellow/Tan	Clear	White	Vapor cloud production during vacuum aspiration.
IRN-78-50%-PA	1MHNO_3:KMnO_4:d	Each 50 drop addition	25	25	-	0.61	Pale Amber	Deep Amber	Greenish/Brown	None	Vapor cloud production during vacuum aspiration.
IRN-78-100%-PA	1MHNO_3:KMnO_4:d	Each 50 drop addition	26	26	-	0.54	Light Yellow/ Amber	Deep Amber. Spotted Deep Purple	Greenish/Brown	None	Some vapor cloud production during vacuum aspiration.
IONAC A-365-50%-PA	1MHNO_3:KMnO_4:d	Each 50 drop addition	22	22	-	2.06	Yellow/White	Greenish/ Purple	Greenish/Brown	None	Vapor cloud production during vacuum aspiration.
IONAC A-365-100%-PA	1MHNO_3:KMnO_4:d	Each 50 drop addition	23	23	-	1.83	Yellow/Tan	Greenish/Brown	Orange/Brown	None	Vapor cloud production during vacuum aspiration.
IRN-78-50%-PA	1MHNO_3:KMnO_4:b	Each 5ml addition	21	21	-	0.67	Light Yellow/ Amber	Deep Brown/ Amber	Greenish/Brown	None	Vapor cloud production during vacuum aspiration.
IRN-78-100%-PA	1MHNO_3:KMnO_4:b	Each 5ml addition	20	20	-	0.75	Yellow Amber	Deep Amber	Greenish/Brown	None	Vapor cloud production during vacuum aspiration.
IONAC A-365-50%-PA	1MHNO_3:KMnO_4:b	Each 5ml addition	20	20	-	2.23	Yellow/White	Med. Greenish/ Purple	Greenish/Brown	None	No vapor production.
IONAC A-365-100%-PA	1MHNO_3:KMnO_4:b	Each 5ml addition	20	21	-	1.84	Yellow/Tan	Light Brown	Brown	None	Vapor cloud production during vacuum aspiration and funnel wall condensate.
IRN-78-100%-EDTA	1MHNO_3:d	Each 50 drop addition	19	25	-	0.50	Light Amber	Yellow/White	Clear	White	No vapor production. Liquid in resin slurry initially white. Following vacuum aspiration a white precipitate remains distributed throughout the resin bed.
IRN-78-100%-EDTA	1MHNO_3:b	Each 5ml addition	21	25	-	0.62	Orange/Amber	Yellow/Cream	Clear	White	Vapor cloud production during vacuum aspiration; milky colloidal precipitate material in resin bed following vacuum aspiration.

Table 2.6 Chemical interactions between nitric acid/potassium permanganate combinations and vacuum-aspirated anion exchange resins loaded with decontamination reagents. (Cont'd)

Resin Type, Organic Acid & Percent Loading	Added Chemical & Method of Addition: bulk (b) or drops (d)	Vacuum Aspiration Performed Following:	Initial Resin Bed Temperature (°C)	Maximum Resin Bed/Slurry Temp. Measured (°C)	pH		Color				General Observations
					Resin Bed Slurry	Eluate	Initial Resin Bed Slurry	Final Resin Bed Slurry	Final Eluate	Precipitate Color	
IONAC A-365-100%-EDTA	$3MHNO_3$:d	Each 50 drop addition	21	26	-	0.21	Yellow/Cream	Yellow/Cream	Clear	White	Vapor cloud production during vacuum aspiration; milky solution precipitates material in resin bed following vacuum aspiration.
IONAC A-365-100%-EDTA	$3MHNO_3$:b	Each 5ml addition	22	26	-	0.22	Yellow/Cream	Yellow/Cream	Clear	White	Vapor cloud production during vacuum aspiration; milky solution precipitates material in resin bed following vacuum aspiration.
IRN-78-100%-EDTA	$3MHNO_3$:$KMnO_4$:d	Each 50 drop addition	23	24	-	0.58	Orange/Amber	Darker Orange/ Amber	Clear	White	No vapor production; filtering flask cold.
IRN-78-100%-EDTA	$3MHNO_3$:$KMnO_4$:b	Each 5ml addition	23	23	-	0.54	Orange/Amber	Yellow/White	Clear	White	Vapor cloud production during vacuum aspiration.
IONAC A-365-100%-EDTA	$3MHNO_3$:$KMnO_4$:d	Each 50 drop addition	24	24	-	1.81	Yellow/Cream	Darker Yellow/ Cream	Clear	White	Vapor cloud production; milky solution precipitates material in resin bed following vacuum aspiration.
IONAC A-365-100%-EDTA	$3MHNO_3$:$KMnO_4$:b	Each 5ml addition	20	20	-	1.75	Yellow/Cream	Yellow/Cream	Salmon	White	As above.

Table 2.7 Chemical interactions between nitric acid/potassium permanganate combinations and cation resins loaded with ferrous ion.

Resin Type, Organic Acid & Percent Loading	Added Chemical & Method of Addition: bulk (b) or drops (d)	Vacuum Aspiration Performed Following:	Initial Resin Bed Temperature (°C)	Maximum Resin Bed/Slurry Temp Measured (°C)	pH		Color				General Observations
					Resin Bed Slurry	Eluate	Initial Resin Bed Slurry	Final Resin Bed Slurry	Final Eluate	Precipitate Color	
VACUUM ASPIRATED RESIN											
IRN-77-100%-$FeSO_4$	1MHNO_3:d	Each 50 drop addition	23	23	-	0.07	Amber	Amber	Yellow/ Green	None	No vapor production; eluate changed color from yellow to dark brown/green (~15 mins).
IRN-77-100%-$FeSO_4$	1MHNO_3:b	Each 5ml addition	20	20	-	0	Amber	Amber	Green/Brown	None	No vapor production; eluate changed color from light brown to deep green/brown to light brown, very strong acid odor (HNO_3).
IRN-77-100%-$FeSO_4$	1MHNO_3:d	Each 50 drop addition	25	25	-	0.05	Amber	Amber	Green/Brown	None	No vapor production; eluate initially clear changing to green/brown and finally light brown, HNO_3 odor very strong.
IRN-77-100%-$FeSO_4$	1MHNO_3:b	Each 5ml addition	26	26	-	0	Dark Amber	Dark Amber	Green/Brown	None	No vapor production; eluate changes colors from mod. green/brown to darker green/ brown to clear, strong HNO_3 odor.
IRN-77-100%-$FeSO_4$	1MHNO_3:$KMnO_4$:d	Each 50 drop addition	26	27	-	0.76	Medium Amber	Medium Amber	Violet	None	Vapor cloud production during vacuum aspiration, eluate stays same color.
IRN-77-100%-$FeSO_4$	1MHNO_3:$KMnO_4$:b	Each 5ml drop addition	26	26	-	0.80	Amber	Lighter Amber	Violet	None	As above.
OVEN-DRIED RESIN											
IRN-77-100%-$FeSO_4$	1MHNO_3:d	Each 100 drop addition	24	46	-	0	Dark Amber	Dark Amber	Light/Brown	None	No vapor generation, strong HNO_3 odor.
IRN-77-100%-$FeSO_4$	1MHNO_3:b	Each 5ml addition	25	36	-	0	Dark Amber	Medium Amber	Light/Brown	None	As above.
IRN-77-100%-$FeSO_4$	1MHNO_3:$KMnO_4$:d	Each 75 drop addition	20	22	-	0.54	Amber	Amber	Purple	None	Vapor cloud production during vacuum aspiration, no reactions.
IRN-77-100%-$FeSO_4$	1MHNO_3:$KMnO_4$:b	Each 5ml addition	24	24	-	0.53	Amber	Amber	Violet	None	As above.

3. CORROSION OF CONTAINER MATERIALS BY WASTE RESINS

This task was initiated to evaluate the compatibility of a range of container materials with a simulated decontamination resin waste. The materials include Ferralium 255 (a duplex stainless steel), TiCode-12 (a dilute titanium alloy), Types 304 and 316 stainless steel, carbon steel, and high-density polyethylene. The carbon steel coupons were added after the first irradiation cycle when some of the original specimens were deemed surplus and removed to provide space. Thus, the carbon steel specimens were exposed to resins which had been pre-irradiated to approximately 5×10^7 rad.

The resin decontamination waste chosen for this task contains LOMI reagents. The reagents promote rapid dissolution of surface oxides by changing the oxidation state of the metal ions, e.g., Fe(III) to Fe(II). By definition, LOMI reagents contain 1) a reducing metal ion and 2) a chelating ligand [Bradbury, 1982]. The vanadous picolinate/formate system is one such reagent which has been successfully applied to full scale reactor decontamination. Because of its superior decontamination capability and the relative nonaggressiveness of the medium, it is one of the most important reagents for present decontaminations. The simulated LOMI resin waste used in this study consists of two volumes of IONAC A-365 anion resin to one volume of IRN-77 cation resin. The IONAC A-365 is loaded with both picolinate and formate ions, whereas, the IRN-77 is always in the as-received H^+ form. The initial moisture content of the mixed bed resin was 47.3 percent by weight. Full details of the resin preparation procedure are given elsewhere [Adams and Soo, 1988].

To check how corrosion is influenced by gamma irradiation (which is present in most types of low level waste) and by the presence of organic reagents on the resin, four types of corrosion test were initiated:

a) corrosion in mixed-bed resins with the anion component loaded with picolinate/formate; cation resin in the H^+ form;

b) corrosion in as-received mixed-bed resins (i.e., anion resin in the hydroxide; cation resin in the H^+ form;

c) similar to (a) but in the presence of a gamma field of about 1×10^4 rad/h; and

d) similar to (b) but in the presence of a gamma field of about 2×10^4 rad/h.

The four resin beds were contained in glass liners measuring 7.0 cm ID × 30.5 cm in height. The metallic specimens were placed horizontally in the resins in two layers, one resting in the flat base of the glass liner and the other close to the resin surface.

The high density polyethylene (Marlex CL-100) specimens were made from strips measuring 10.2 × 1.25 × 0.32 cm. They were bent into a "U-bend" configuration by bending them and fastening the two ends with steel nuts and bolts. In the molding of the drum from which the specimens were cut, one side of the drum becomes oxidized by air. When the oxidized mateiral is on the outer surface of a U-bend specimen, cracks are formed because of the lower ductility. When the non-oxidized material is on the outer bend

surface, no cracking is present. Crack propagation during testing was studied for samples with both oxidized (cracked) surfaces and non-oxidized (uncracked) surfaces on the U-bend specimens. The polyethylene specimens were placed between the two metallic specimen layers with the apex of each U-bend facing upward.

For the two systems being irradiated, the glass liners containing the resins and specimens were enclosed in sealed stainless steel pressure vessels connected to a pressure gauge/data logger system. A vacuum system was also connected to the vessel to facilitate purging and the removal of gas samples for analysis. Figure 3.1 shows a schematic of the system.

For the unirradiated tests, the liners containing the specimens were sealed with plastic foil and placed in a refrigerator at 10°C, the gamma irradiation temperature.

3.1 Gas Generation During Irradiation

In the previous Annual Report [Adams and Soo, 1988], it was shown that irradiation of the resin/specimen system causes an initial 20 percent decrease in vessel pressure. This was attributable to the loss of oxygen from the air cover gas by the well-known gamma-induced resin oxidation mechanism. Thereafter, the system pressure increased in a linear fashion until the specimens were removed for examination or until a gas sample was taken for analysis.

Table 3.1 gives gas compositions measured from samples taken periodically from the irradiated resin vessels. For the unloaded control resin the corrosion specimens were examined after an accumulated dose of 4.9×10^7 rad. However, gas analyses were not made at this time. During the second irradiation cycle between day 150 and day 210, an additional incremental dose of 2.9×10^7 rad was administered. The gas sample taken on September 28 was analyzed and found to have little remaining oxygen. Significant amounts of hydrogen and carbon monoxide were generated and some nitrogen was lost. After opening the vessel to examine the corrosion specimens and subsequent repacking of the column, a third irradiation cycle was carried out giving an additional gamma dose of 2.3×10^7 rad. The air cover gas composition changed in a very similar manner to that observed in the previous cycle.

In the case of LOMI-loaded resins, nitrogen appeared to have been generated during the first irradiation cycle after a dose of 2.3×10^7 rad (Table 3.1). Oxygen was again lost and hydrogen was generated. Hydrogen formed at about half the rate compared to the non-loaded resins. Possibly, the nitrogen originated from a breakdown of the picolinic acid on the anion resin. However, this is highly speculative. After a second irradiation dose of 2.9×10^7 rad, the gas composition became more similar to those for non-loaded resins insofar that nitrogen levels decrease, oxygen was essentially depleted, and large amounts of hydrogen were formed. Carbon monoxide levels, however, were quite low (5 percent by vol.).

Data were also obtained on the moisture contents of the irradiated and control resin beds as a function of time. Table 3.2 shows the percent water for resin samples taken from

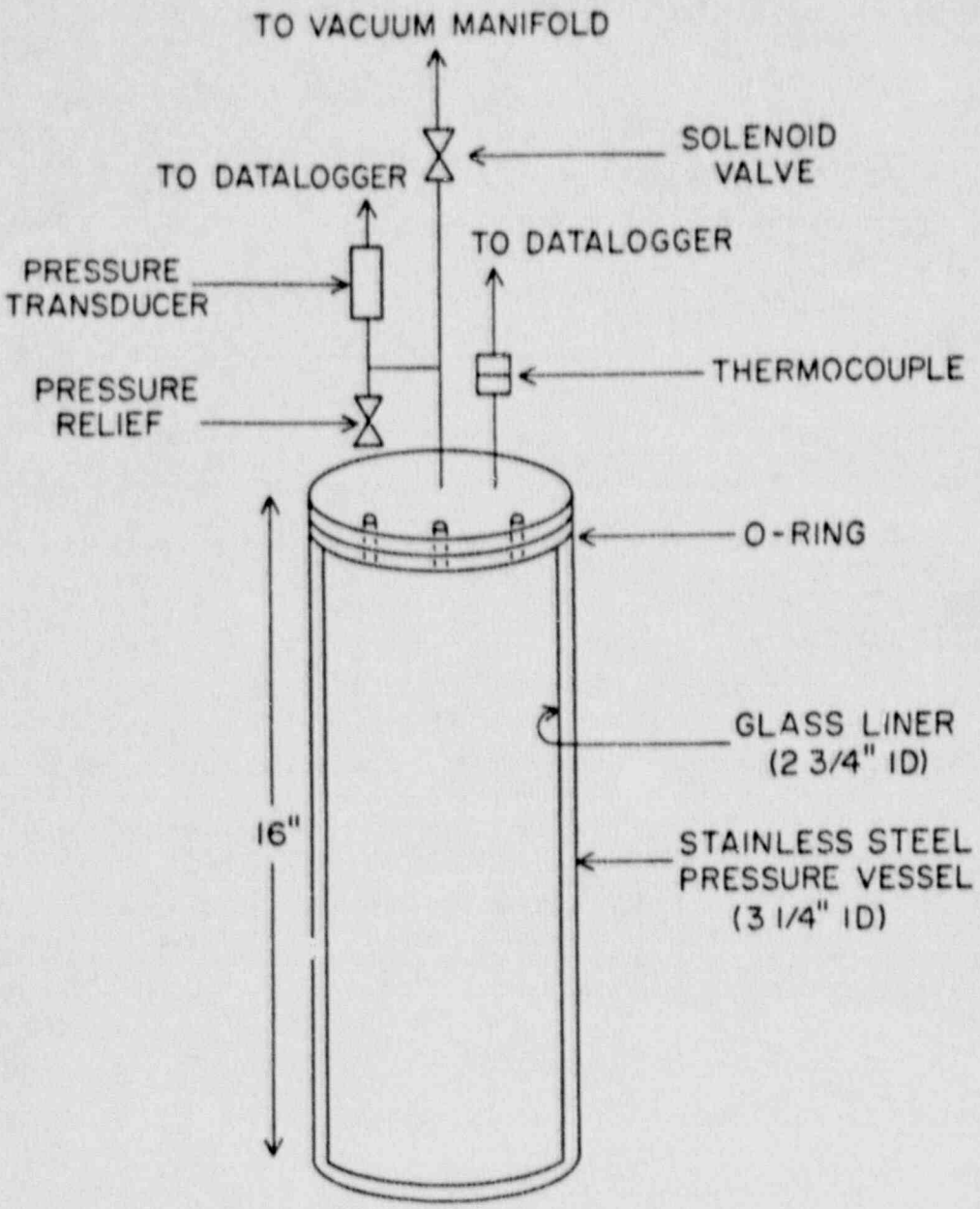

Figure 3.1 Line drawing of irradiation pressure vessel used for container corrosion studies.

Table 3.1

Composition of gases in sealed ion-exchange resin columns after gamma irradiation

Resin Type	Date Gas Sampled	Incremental Gamma Dose (rad)[1]	Composition of Gas in Irradiation Vessel (v/o)					
			N_2	O_2	H_2	Ar	CO	CO_2
Unloaded Control Resin	3/4/87 (start date)	0	78.1[2]	20.9	0.01	0.93	—	0.03
	6/2/87	4.9×10^7	[3]					
	9/28/87	2.9×10^7	58.8	0.25	23.0	0.87	17.1	ND[4]
	12/8/87	2.3×10^7	59.1	0.31	18.8	0.73	21.0	ND
LOMI-Loaded Resin	3/4/87 (start date)	0	78.1[2]	20.9	0.01	0.93	—	0.03
	6/2/87	2.3×10^7	86.8	1.07	10.7	0.88	ND	0.51
	9/28/87	2.9×10^7	58.7	0.46	32.9	0.81	5.25	1.83

[1] Note that these doses are administered during periods between the opening of the irradiation vessels to examine the corrosion specimens. Upon repacking the samples and sealing the vessels, the atmosphere in the vessel is, again, air.

[2] Composition of gas in the vessel at the beginning of the tests is that of laboratory air. Data taken from Handbook of Chem. and Phys., CRC Press, 1981-1982.

[3] Corrosion specimens examined but gas analyses not performed.

[4] Not detected.

Table 3.2

Percent moisture contents in resin columns used for HIC corrosion tests[1]

Resin Sampling Location	Date Sampled and Accumulated Gamma Dose (rad)					
	Unirrad. Unloaded Control Resin[2]		Irrad. Unloaded Control Resin[2]		Unirrad. LOMI-Loaded Resin[3]	Irrad. LOMI-Loaded Resin[3]
	9/24/87	12/8/87	6/15/87 (4.9×10^7 R)	12/8/87 (1.1×10^8 R)	9/24/87	9/24/87 (5.2×10^7 R)
Top	45.1	46.1	48.3	47.6	38.5	44.6
Middle	47.6	46.9	48.4	47.7	42.6	44.8
Bottom	50.7	50.3	48.5	48.8	43.8	46.7

[1] Based on weight change measurements after heating resins as 110°C for 5 days.

[2] Starting moisture level on 3/4/87 was 52.7%.

[3] Starting moisture level on 3/4/87 was 47.3%.

the top, middle, and bottom sections of the columns during the periodic examination of the corrosion specimens. The resins were slightly wetter in the lower sections, as evidenced by their tendency to clump together. Obviously, free water settles under gravity and large droplets and films of moisture were always observed on the base of the glass liners containing the resins.

There was also a small overall loss of moisture compared to the starting levels. This is probably connected with gravity settling of water and also evaporation and precipitation of water on the vessel walls enclosing the gas space above the resin bed. Radiolysis of water may also make a contribution to water loss.

After gamma irradiation to about 5×10^7 rad, the loaded and control ion exchange resins were examined for radiolytic degradation. Three samples of approximately 10 g of mixed-bed resin from the top, middle, and bottom sections of the vessels were removed and mixed with 20 mL of deionized water. The solutions were examined for pH, total carbon and picolinic acid. The results showed that there were negligible differences between the irradiated and unirradiated resin mixtures [Adams and Soo, 1988]. The organic acids in solution represent about 3% of the picolinic acid initially loaded on the resin.

3.2 Corrosion Analysis

The corrosion coupons used in the study were initially intended to be high-integrity container materials only. Currently, Ferralium-255 (a duplex stainless steel), and a steel-fiber-reinforced polymer-impregnated concrete are the only NRC-licensed high-integrity container (HIC) materials. Attempts to obtain samples of the latter material from the manufacturer were not successful and the only HIC materials studied were high density polyethylene Ferralium-255. Because of available space in the test vessels, it was decided that non-HIC materials would also be studied since they were available as surplus samples from other programs. They included Types 304 and 316 stainless steel, TiCode-12 a dilute titanium alloy, and mild carbon steel. Table 3.3 gives the nominal chemistries of the metallic materials selected.

The Ferralium 255 was donated by the Cabot Corp., Kokomo, IN. It was the only alloy studied which included both weld and base material. The weld was made with a shielded

Table 3.3

Composition of test materials (Wt. %)

Material	C	Cr	Ni	Mo	Cu	P	S	Si	Mn	Fe	Ti
Fe-255	0.02	25.8	5.8	3.3	1.9	0.02	0.006	0.6	0.8	Bal.	—
Ti-12	0.1m[(1)]	—	0.8	0.3	—	—	—	—	—	0.3m	Bal.
T304 SS	0.08m	18.0	8.0	—	—	—	—	—	2.0m	Bal.	—
T316 SS	0.08m	17.0	13.0	2.0	—	—	—	—	2.0m	Bal.	—
C steel	0.18	—	—	—	—	—	0.05m	—	0.8	Bal.	—

Note: [(1)]m denotes maximum permissible concentration.

metal arc process using a filler rod enriched by 2% nickel compared to the base metal composition. The samples measuring about 3/8 inch wide and 2 inches long (0.95 × 5.08 cm) were cut across the weld, with the weld in the center of the sample. The coupons were initially tested in the as-welded condition but, after the first test period, were pickled for 2 hours in a solution of 20% HNO_3 and 5% HF in water at 150°F (66°C) in an attempt to chemically polish the metal surface so that corrosion effects could be more clearly observed. This was unsuccessful. After trying other chemical polishing procedures, with little improvement, it was decided to mechanically polish the Ferralium to a mirror finish using an alumina-based polishing compound.

The TiCode-12 specimens were cut from the as-received sheet and chemically polished in a solution of nitric acid, hydrofluoric acid and water (1:1:50) at 22°C for 30 seconds and rinsed in water.

Sheets of approximately 1/64 inch thick (0.04 cm) Types 304 and 316 stainless steel were received from Somers Thin Strip, Waterbury, CT. The Type 304 sheet was cut into 1/2 inch squares (1.27 cm) and the Type 316 sheet was cut into 3/8 × 1 inch rectangles (0.95 × 2.54 cm). The as-rolled and annealed surfaces were bright, so no further preparation was necessary even though some specimens displayed some fine surface scratches.

All samples were stamped with an identifying number. Ultrasonic cleaning in methanol for 5 minutes was used for degreasing, followed by air drying. Dimensions and weights were recorded for every sample prior to testing.

Samples of HDPE were obtained from the sidewall of a Marlex CL-100 container prepared by rotary molding. During this process, the Marlex resin is heated in a metal mold to about 300°C, often by high-temperature forced air. By rotating the mold about two independent orthogonal axes, a uniform wall thickness is achieved. The molding process is completed by cooling the mold by water. As a result of this procedure, the internal surfaces of the container have a thin oxidized layer of about 5 microns, whereas the opposite surfaces in contact with the mold are not significantly affected [Terselius, 1982; Soo, and others, 1986]. Test samples measured 4 × 1/2 × 1/8 inch thick (10.16 × 1.25 × 0.32 cm). U-bend samples were constructed from the strips by drilling a hole 1/2 inch (1.25 cm) from each end, bending the strip back on itself and securing the two ends with a steel nut and bolt. Half of the bends were made with the oxidized surface facing outward and half were made with the opposite nonoxidized surface facing outward. The oxidized surfaces in tension (facing out) crack immediately under ambient conditions; the positions and approximate depths of the cracks were noted by a simple drawing. The non-oxidized surfaces remain uncracked after bending.

Figure 3.2 shows samples of starting materials. The Ferralium is shown in the original as-welded state as well as the metallurgically polished condition. Corrosion results for each material are discussed below.

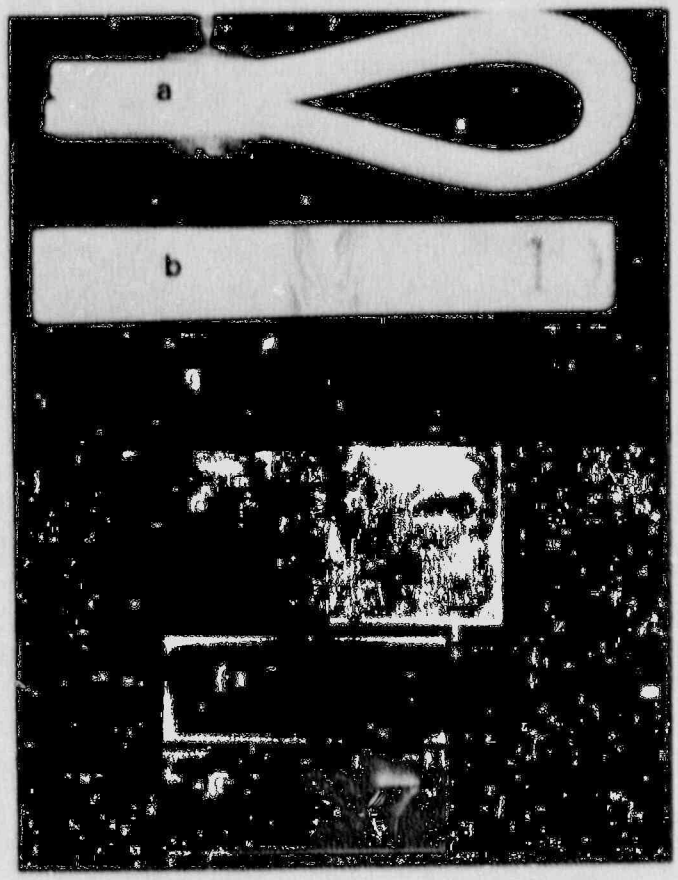

Figure 3.2 Appearance of starting materials for corrosion tests: (a) high-density polyethylene, (b) as-welded Ferralium 255, (c) polished Ferralium 255, (d) polished carbon steel, (e) as-received Type 304 SS, (f) polished TiCode-12, (g) as-received Type 316 SS. Mag. 1.5×.

3.2.1 Type 304 Stainless Steel

At this time, data are available for metal specimens irradiated to 2×10^8 rad in LOMI-loaded resins and to 1×10^8 rad in as-received resins. Data are also available for the unirradiated counterparts of these systems.

Figure 3.3 shows the typical appearance of some stainless steel coupons removed from a resin bed. Clumps of resins usually adhere to the surfaces because of surface tension forces created by moisture trapped between individual resin beads and the metal. The arrow shows a location where a bead had originally resided leaving behind an area of spot corrosion. These are more clearly seen after a particular specimen (Number 22) was cleaned in alcohol after two successive irradiation cycles in as-received mixed-bed resin (Figure 3.4). Corrosion spots formed during the first irradiation do not grow during the second irradiation since new contact points were formed between the resin beads and the metal. It was noticed that the resin beads causing the corrosion turned to an orange-red color indicating that the corrosion mechanism is caused by ferrous ion exchange between the metal surface and a cation resin bead. The process is encouraged by the presence of the liquid interface between the resin and the metal. Throughout this study, for all materials, the appearances of the top and bottom surfaces were similarly corroded. The exception was for the bottom layer of samples whose bottom surfaces were in contact with the base of the glass liner. Spot corrosion was not seen in this case.

Figure 3.5 shows an enlarged view of a corrosion spot. Etching of individual grains shows that the corrosion process is dependent on grain orientation.

Figure 3.6 shows the effects of gamma irradiation on the corrosion of Type 304 stainless steel in contact with as-received resins. None of the unirradiated specimens (Numbers 2, 9, 14, 19) were attacked by the resin environment after 488 d of exposure. The surfaces remained bright and clean with only the original scratches and marks from the manufacturers rolling operations being visible. On the other hand, irradiation to 2×10^8 rad usually caused extensive spot corrosion. The exception was specimen 20 which showed only a small patch of attack indicated by the arrow in Figure 3.6. This specimen was from the lower layer of specimens resting on the base of the glass liner. Reasons for the lack of attack by the resins are not known, but it could possibly be caused by some none uniform surface cleaning process at the manufacturers which could have passivated the surface locally.

Examination of Figures 3.4 and 3.6 show three views of specimen 22 which was given three separate irradiation increments. It may be seen that the density of corrosion spots grew with each cycle which, as mentioned above, was caused by resin beads making new contact points on the surfaces of the specimens as they were repacked into the resin bed for retesting. Old corrosion spots did not noticeably grow in size without additional resin bead contact.

In Figure 3.7 are shown specimens which had been emplaced in LOMI-loaded resins. In the absence of irradiation, no attack occurred after 412 d. Irradiation for the same time

Figure 3.3 Mixed-bed ion-exchange control resins adhering to Types 304 and 316 stainless steel specimens (top and bottom resp.) after irradiating to 4.9×10^7 rad.

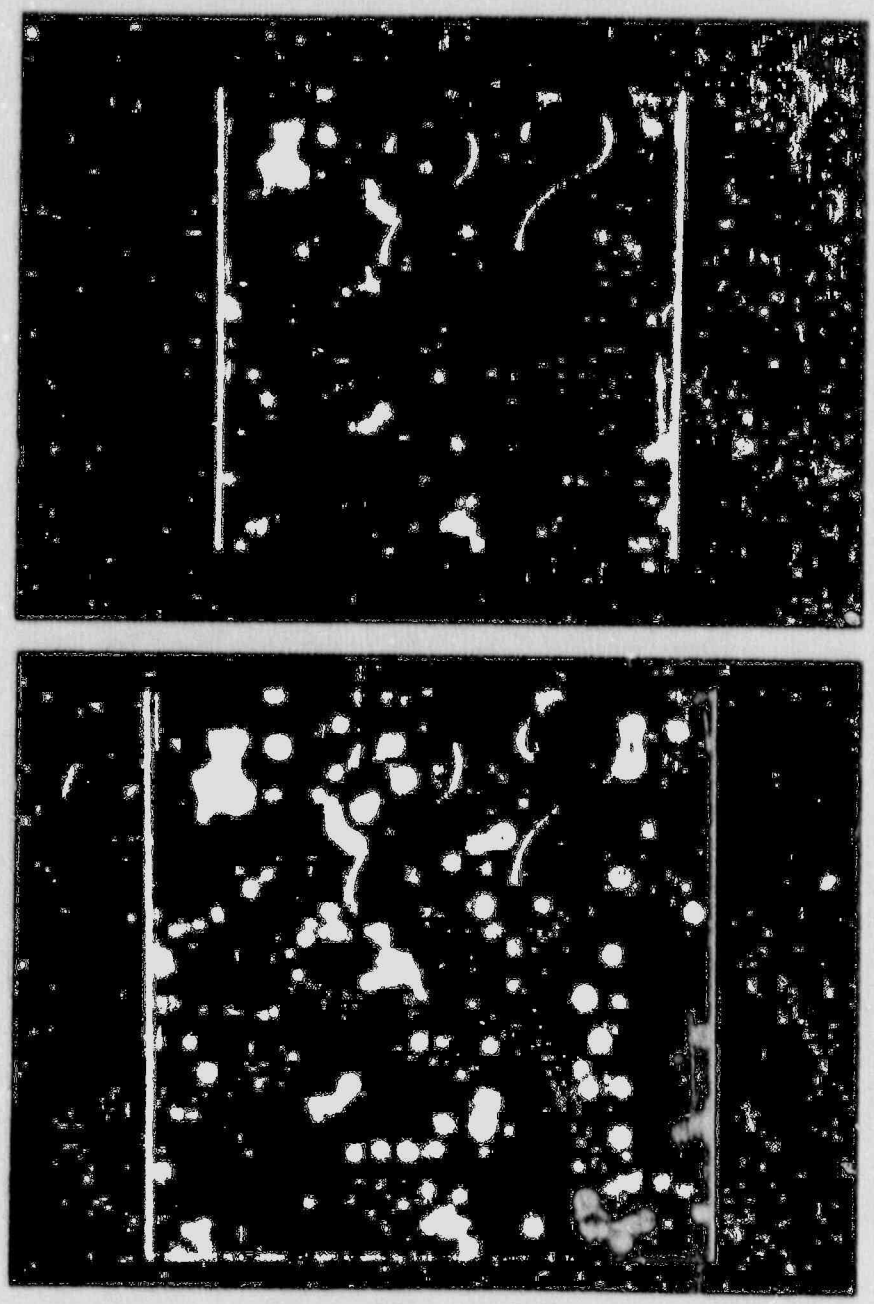

Figure 3.4 Type 304 stainless steel specimen exposed to mixed-bed control ion-exchange resins. Top micrograph shows specimen after a total gamma dose of 4.9×10^7 rad; bottom view shows same specimen after an additional dose of 5.2×10^7 rad. Magnification 4× and 5×, respectively.

Figure 3.5 Corrosion spot at a cation resin contact point with Type 304 stainless steel. Resins loaded with LOMI reagent and irradiated for 412 d to 1.0×10^8. Magnification 200×.

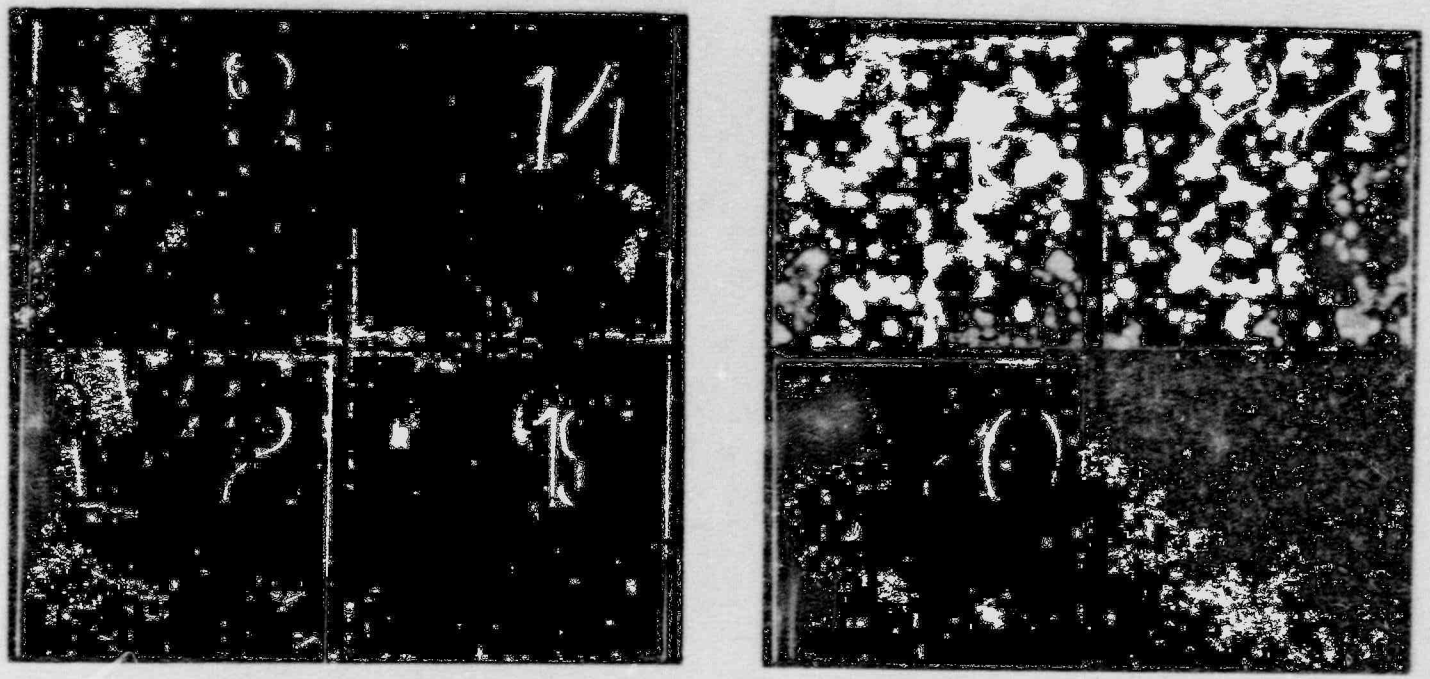

Figure 3.6 Effect of gamma irradiation on the corrosion of Type 304 stainless steel by as-received mixed-bed resins. Samples on the left were exposed for 488 d without irradiation; samples on the right were irradiated for 447 d to 2.1×10^8 rad. Note the reduced attack in specimen 20 shown by arrow. Magnification 2.7×.

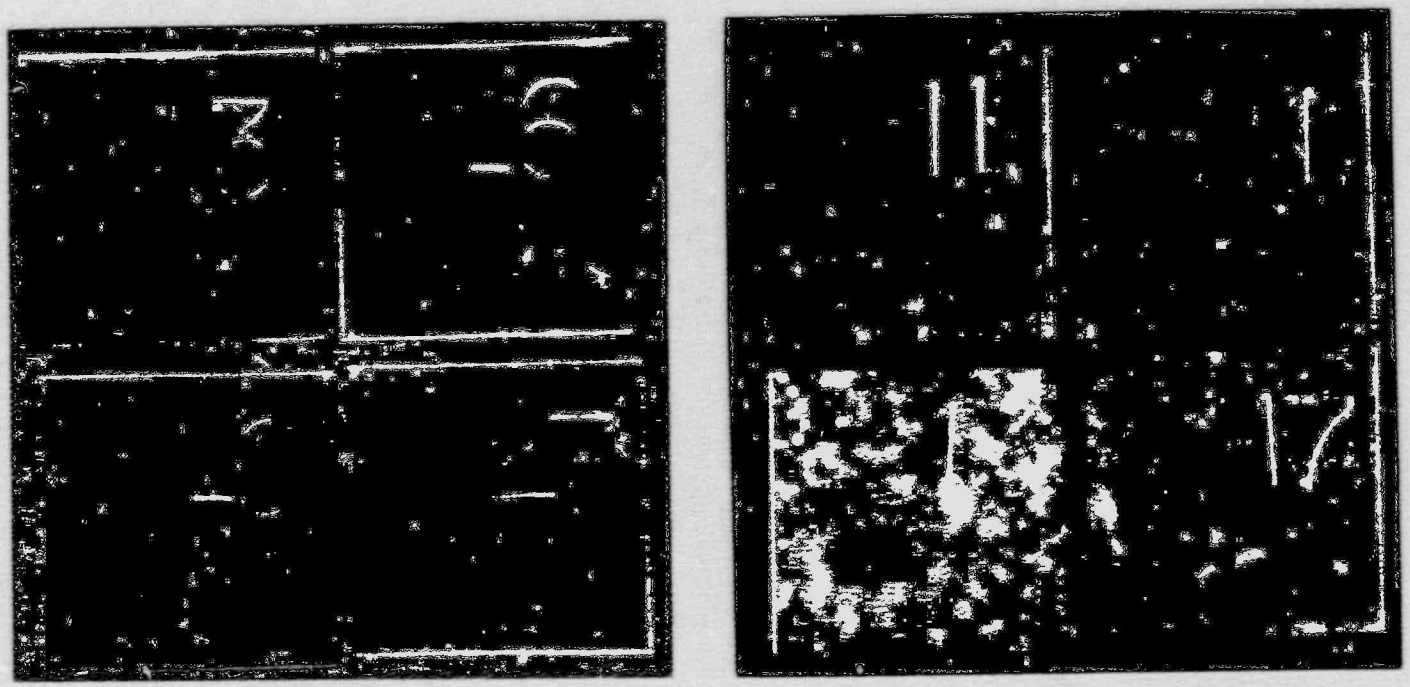

Figure 3.7 Effect of gamma irradiation on the corrosion of Type 304 SS by mixed-bed resins loaded with picolinate/formate decontamination reagents. Samples on the left were exposed for 412 d without irradiation; samples on the right were irradiated for 412 d to 1.0×10^8 rad. Magnification 2.7×.

period to a dose of 1×10^8 rad, however, caused a large amount of spot corrosion. One specimen from the bottom layer (Number 13) showed more corrosion than the other three.

When the irradiated specimens in Figure 3.6 and 3.7 are compared, there does not appear to be any definitive conclusion that can be drawn with respect to the influence of the LOMI reagent since there were significant variations in the degree of corrosion in specimens exposed in the same system. For example, Specimen 20 showed little attack compared to Specimens 18 and 22 (Figure 3.6). Also, Specimen 13 in Figure 3.7 showed more attack than the other three samples. It is clear, however, that for the test conditions used in this study, as received or LOMI-loaded resins did not corrode Type 304 stainless steel. If gamma irradiation is present, both types of resin will lead to spot attack. Thus, LOMI reagent is not necessary for the corrosion process.

3.2.2 Type 316 Stainless Steel

Type 316 stainless steel is known to show a similar corrosion trend to Type 304 but is expected to display noticeably higher corrosion resistance. In Figure 3.8 it is seen that there was no attack on Type 316 after exposure to unirradiated as received resins for 488 d. Nor was there attack after an accumulated 447 d irradiation to 2.1×10^8 rad. This is in contrast to Type 304 stainless steel which underwent corrosion in irradiated as-received resins (Figure 3.6).

In the presence of LOMI-loaded resins, Type 316 stainless steel only corroded in the presence of radiation (Figure 3.9). The corrosion spots were small and regularly spaced and very similar to those for Type 304 stainless steel irradiated under identical conditions (Figure 3.7).

3.2.3 Carbon Steel

The carbon steel corrosion results for as-received resins are shown in Figure 3.10 for non-irradiated conditions. An exposure of 68 days caused deep "pock marks" to form at points of resin contact which are much deeper than those for stainless steel. After a second corrosion cycle, when an accumulated exposure time of 284 d had elapsed, addition corrosion occurred at new resin contact points. However, the extra corrosion was not very great, indicating that the corrosion kinetics had decreased with time. It was also noted that specimens from the lower layer in the glass liner were more heavily attacked, possibly because of the wetter conditions.

Figure 3.11 shows samples exposed to as-received resins in the presence of gamma irradiation. As was the case for non-irradiated material, there was not a major increase in attack when the corrosion time was increased from 129 d to 344 d. The equivalent gamma doses for these times are 6.2×10^7 and 1.6×10^8, respectively. A comparison between Figures 3.10 and 3.11, furthermore, shows that the corrosion of carbon steel in as-received resins is similar for the irradiated and non-irradiated environments.

For LOMI-loaded resins, Figure 3.12 shows steel irradiated for 208 d to a dose of 5×10^7 rad. The specimen from the bottom layer exhibited large irregular patches of attack

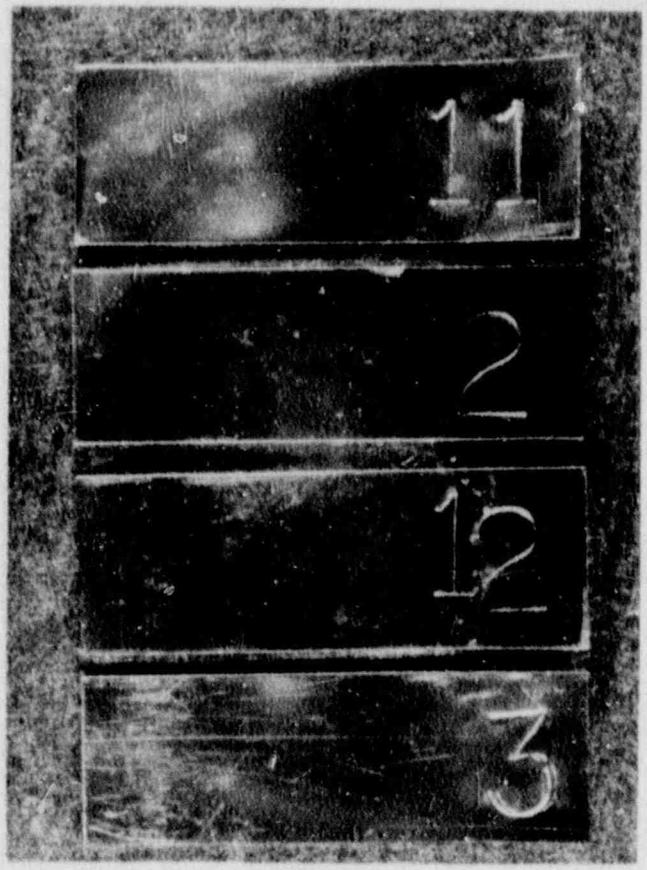

Figure 3.8 Effect of irradiation on the corrosion of Type 316 stainless steel by as-received mixed-bed resins. Top two samples exposed for 488 days without irradiation; bottom two samples irradiated for 488 d to 2.1×10^8 rad. Magnification 2.7×.

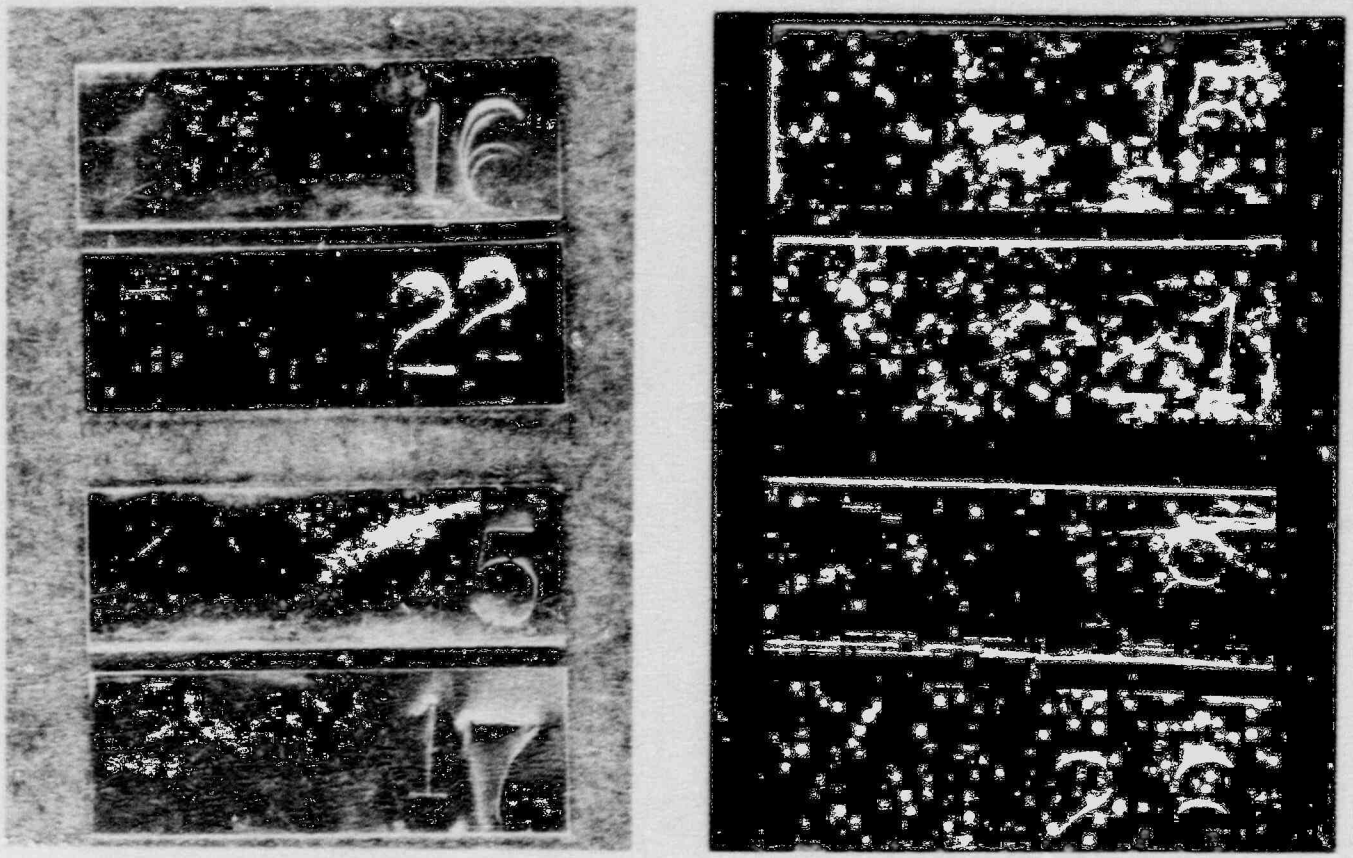

Figure 3.9 Effect of irradiation on the corrosion of Type 316 stainless steel by mixed-bed resins loaded with picolinate/formate decontamination reagents. Samples on the left were exposed for 412 d without irradiation; samples on the right were irradiated for 412 d to 1.0×10^8 rad. Magnification 2.7×.

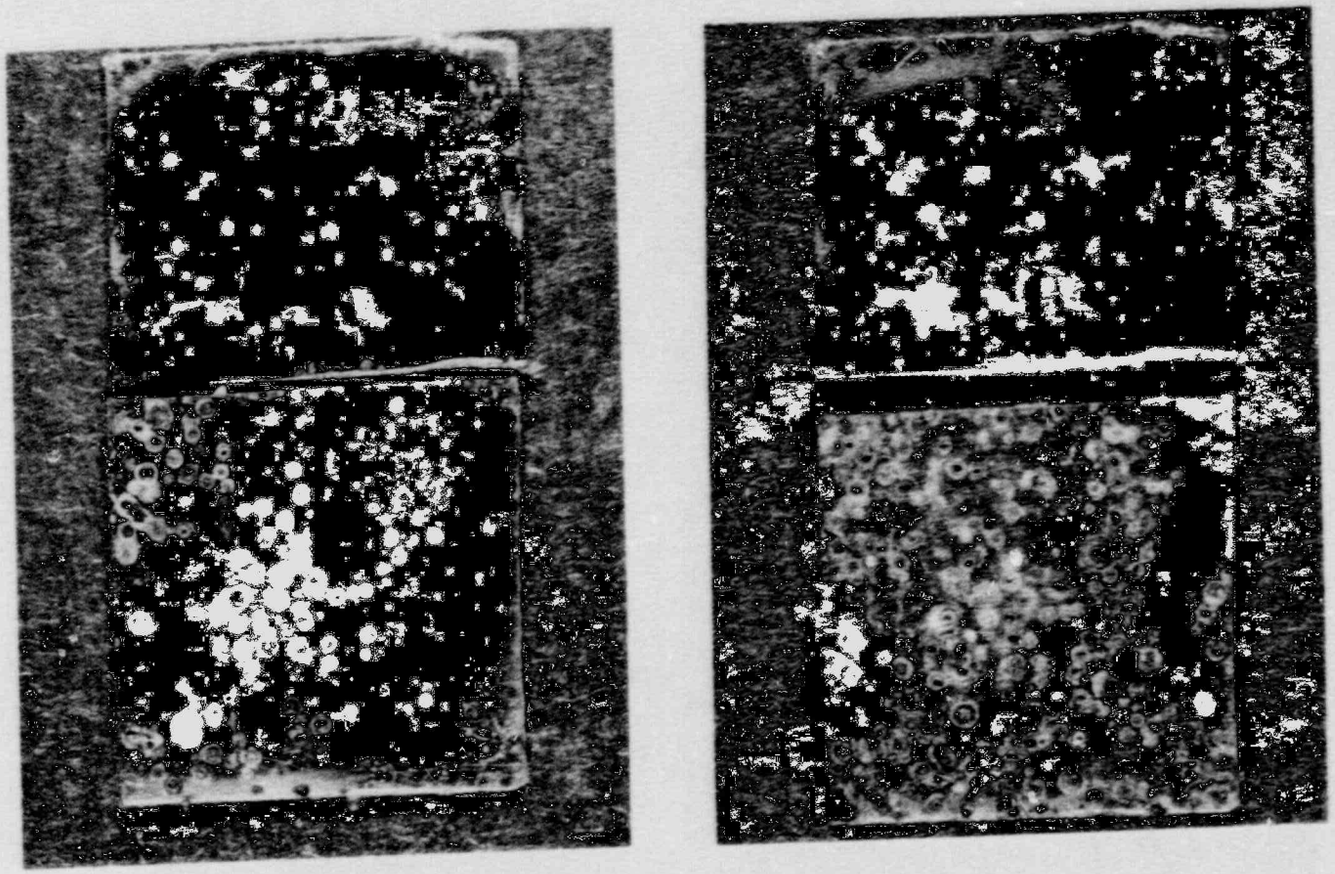

Figure 3.10 Corrosion of two carbon steel specimens by as-received mixed-bed resins. The views on the left show attack after 68 d and those on the right show additional attack after a total exposure of 284 d. Magnification 4×.

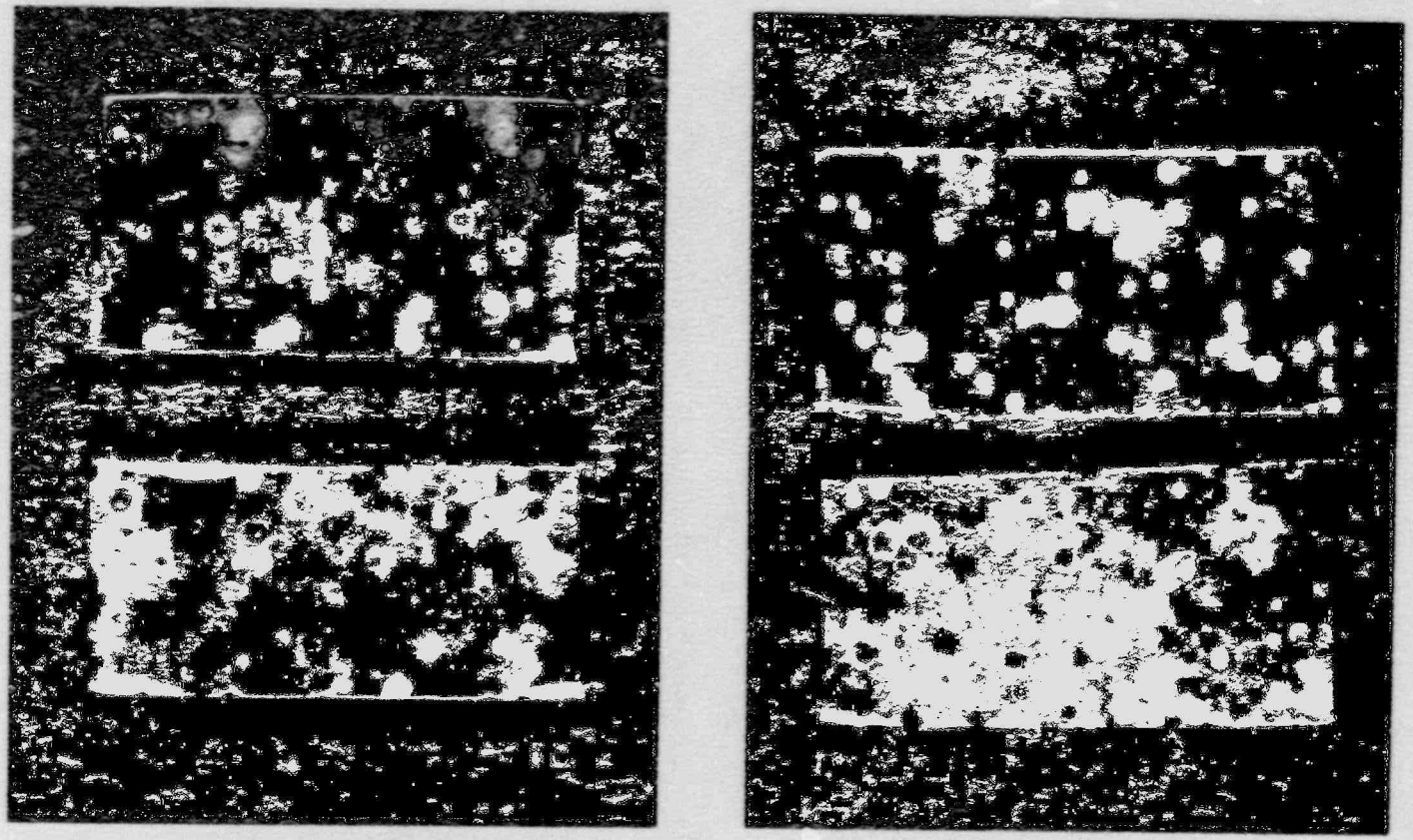

Figure 3.11 Corrosion of carbon steel by as-received mixed-bed resins. Samples on the left were irradiated for 129 d to a dose of 6.2×10^7 rad and samples on the right were irradiated for 344 d to a dose of 1.7×10^8 rad. Magnification 4×.

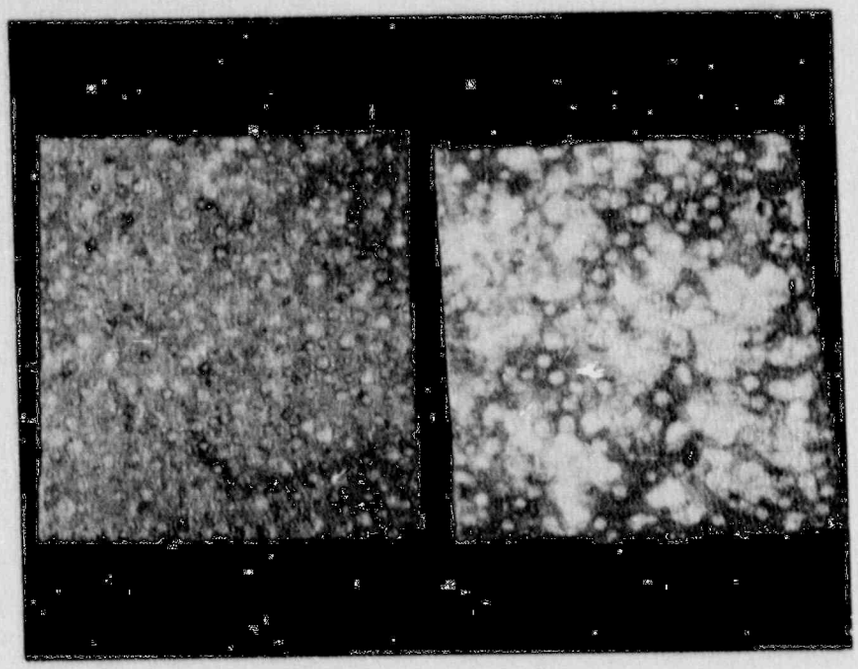

Figure 3.12 Corrosion of carbon steel by mixed-bed resins loaded with picolinate/formate decontamination reagents. Samples irradiated for 208 d to a dose of 5×10^7 rad. Magnification 4×.

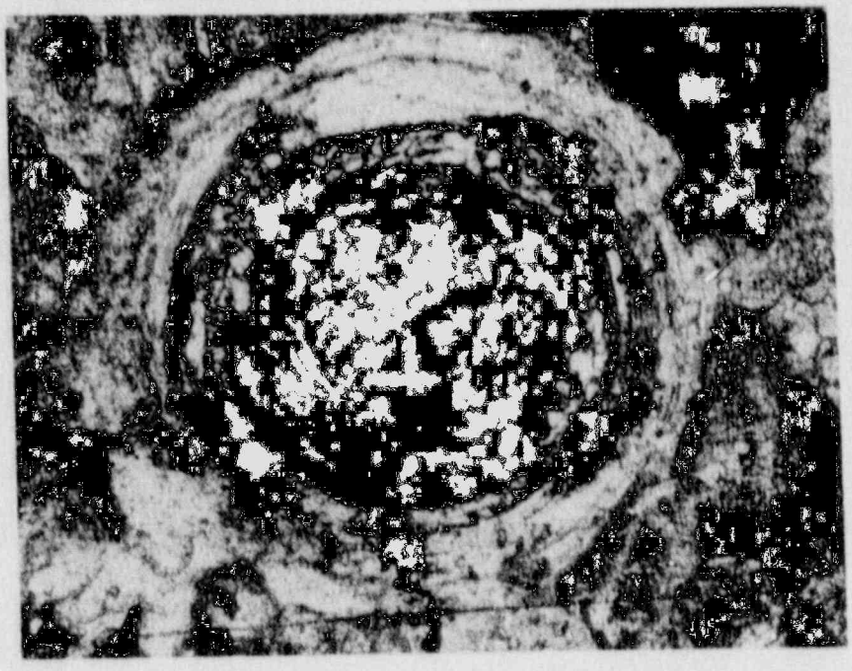

Figure 3.13 Magnified view of corrosion spot on carbon steel exposed to a mixed-bed resins loaded with picolinate/formate decontamination reagent. Sample irradiated to 1×10^8 rad. Magnification 200×.

which is probably connected with the existence of extra moisture which "puddles" on the surfaces of the specimens causing enhanced corrosion. A comparison with the steel specimen in Figure 3.11 that was irradiated to 6.2×10^7 rad in the absence of LOMI reagent, shows no marked effect of the reagent; large blotchy corrosion areas are seen in both resin systems.

An enlarged view of a corrosion pock mark is shown in Figure 3.13. The corroded area is relatively deep compared to stainless steel corrosion spots and concentric layers of corrosion product are observed. It seems that material is transported from the metal / resin bead interface and that the bead embeds itself into the steel surface. Unirradiated carbon steel specimens show similar corrosion effects.

3.2.4 Other Alloys

Ferralium-255 and TiCode-12 did not show significant corrosion under any of the current test conditions. Surfaces remained shiny and little, if any, staining was ever noticed. They are very clearly superior to the austenitic stainless steels with respect to attack by simulated decontamination resin wastes.

3.2.5 High-Density Polyethylene

As described above, polyethylene U-bends were made from flat strips which were bent and held in a U configuration with a steel nut and bolt. When oxidized material is at the apex, it suffered surface cracking. When the unoxidized surface is at the apex, no cracks were formed upon bending. The tests carried out here were to study crack initiation in the unoxidized surfaces, and crack growth and crack initiation in oxidized material, as a function of exposure to the various resin/radiation environments.

To date, no cracks have been observed to initiate in unoxidized polyethylene, even when irradiation was present. For oxidized material, however, there was both crack growth and crack initiation during long-term exposure to as received and LOMI-loaded resins in the unirradiated state (Figures 3.14 and 3.15). Arrows in these figures show locations of crack activity.

In contrast, there was essentially no crack initiation or growth if the resins were irradiated (Figures 3.16 and 3.17). The explanation for this effect is connected with the rapid loss of oxygen in the system because of gamma induced oxidation of the resin bed. It has been shown many times that oxygen is able to react quickly with polymeric materials that are undergoing chain-scission caused by ionizing radiation. Once the oxygen is lost from the system, the degradation of the polymer is greatly retarded [Gillan and Clough, 1981; Soo, and others, 1986].

3.2.6 Summary of Corrosion Results

Table 3.4 summarizes the current status of the container material corrosion effort. After the LOMI-resin system has achieved a radiation dose of 2×10^8 rad (expected in July, 1989), this series of experiments will be completed and a topical report will be prepared.

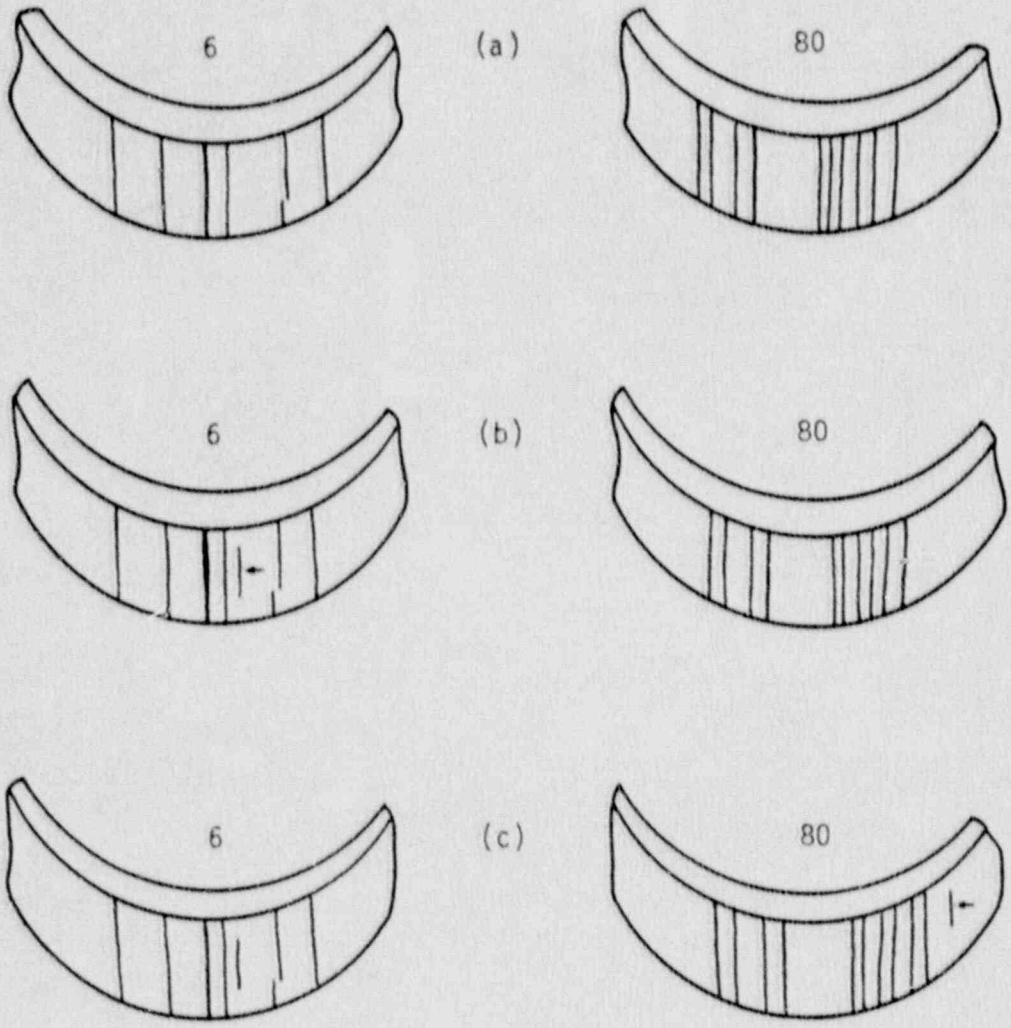

Figure 3.14 Cracking in the oxidized surfaces of Marlex CL-100 HDPE U-bend samples placed in contact with as-received mixed-bed resins; (a) crack patterns at start of testing, (b) crack patterns after 204 d, (c) crack pattern after 403 d. Specimen numbers given above each sketch.

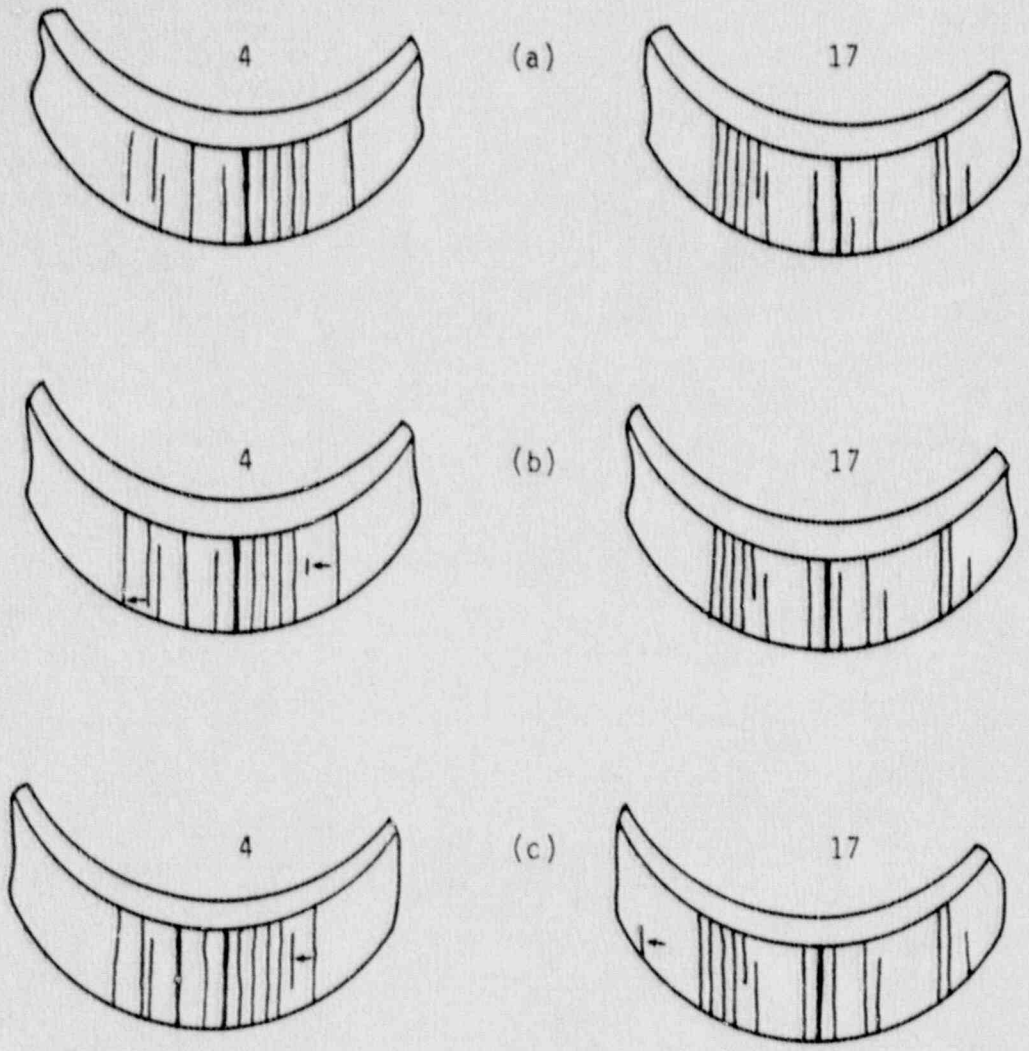

Figure 3.15 Cracking in the oxidized surfaces of Marlex CL-100 HDPE U-bend samples placed in contact with picolinate/formate loaded mixed-bed resins: (a) crack patterns at start of testing, (b) crack patterns after 204 d without irradiation, (c) crack patterns after 420 d. Specimen numbers given above each sketch.

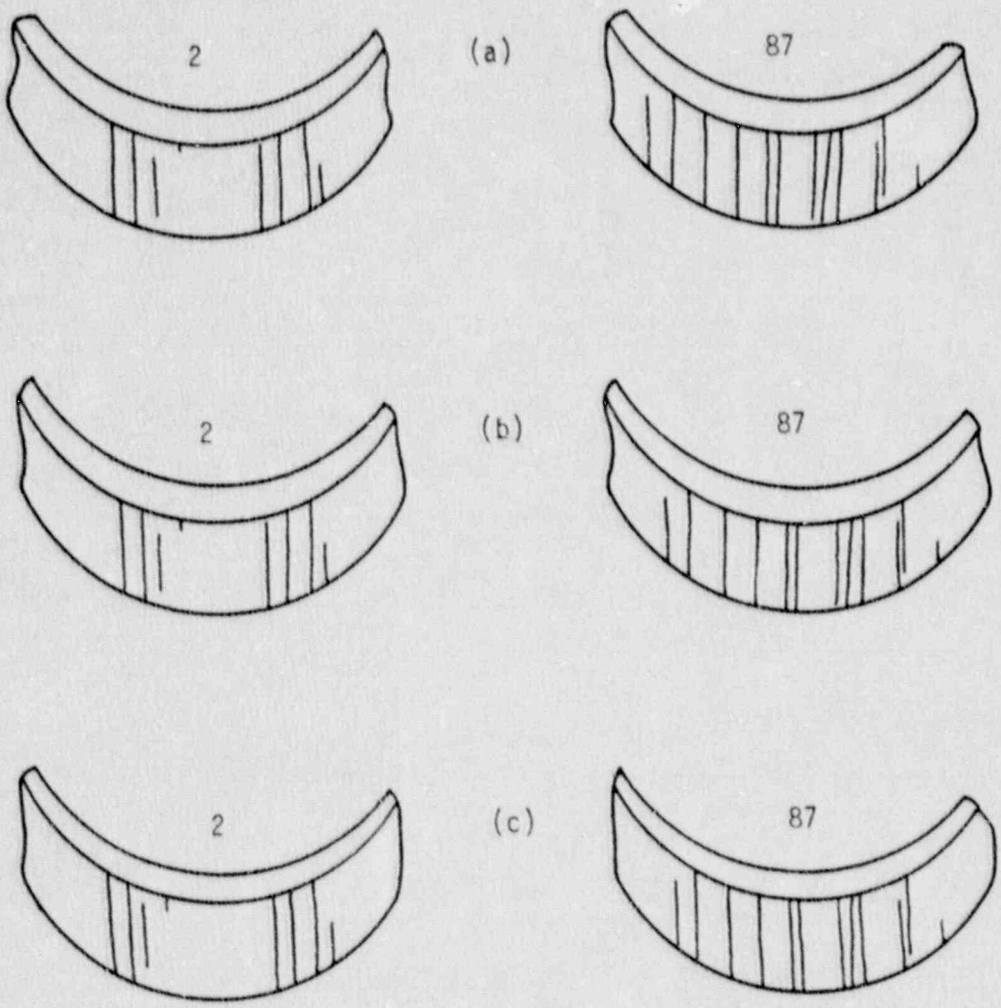

Figure 3.16 Cracking in the oxidized surfaces of Marlex CL-100 HDPE U-bend samples placed in contact with as-received mixed-bed resins; (a) crack patterns at start of testing, (b) crack patterns after irradiating to 4.9×10^7 rad, (c) crack patterns after irradiating to 2×10^8 rad. Specimen numbers given above each sketch.

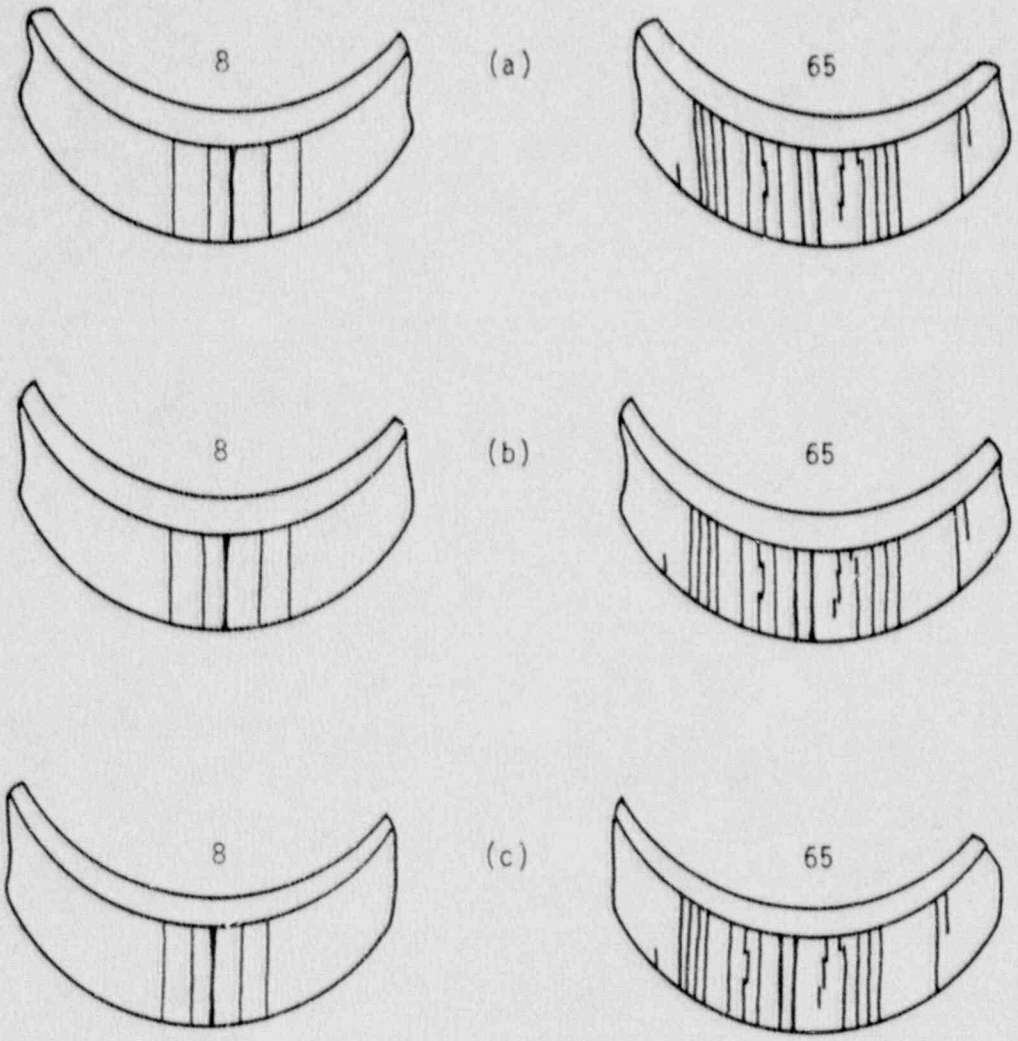

Figure 3.17 Cracking in the oxidized surfaces of Marlex CL-100 HDPE U-bend samples placed in contact with picolinate/formate loaded mixed-bed resins; (a) crack patterns at start of testing, (b) crack patterns after irradiating to 5.2×10^{7} rad, (c) crack patterns after irradiating to 1×10^{8} rad. Specimen numbers given above each sketch.

Table 3.4

Summary of corrosion results for container materials exposed to LOMI decontamination reagent and gamma radiation

Material	Control Resin		LOMI-Loaded Resin	
	Unirradiated	Irradiated	Unirradiated	Irradiated
Carbon Steel	Local pock mark attack during 68 d exposure; additional attack during next 216 d but at slower rate.	Local pock mark attack after 129 d irrad. to 6.2×10^7 rad; additional slower attack during cumulative irrad. of 344 d to 1.65×10^8 rad.	Local pock mark attack during 208 d exposure.	Local pock mark attack during 208 d irrad. to 5×10^7 rad.
T304 SS	No attack during 488 d exposure.	Spot attack during 447 d irrad. to 2.1×10^8 rad.	No attack during 412 d exposure.	Spot attack during 412 d irrad. to 1×10^8 rad.
T316 SS	No attack during 488 d exposure.	No attack during 447 d irrad. to 2.1×10^8 rad.	No attack during 412 d exposure.	Spot attack during 412 d irrad. to 1×10^8 rad.
Ti-12	No attack during 488 d exposure.	No attack during 447 d irrad. to 2.1×10^8 rad.	No attack during 412 d exposure.	No attack during 412 d irrad. to 1×10^8 rad.
Fe-255	No attack during 488 d exposure.	No attack during 447 d irrad. to 2.1×10^8 rad.	No attack during 412 d exposure.	No attack during 412 d irrad. to 1×10^8 rad.
HDPE	Some crack initiation and propagation during 488 d exposure.	No significant crack growth during 447 d irrad. to 2.1×10^8 rad.	Some crack initiation and propagation during 412 d exposure.	No significant crack growth during 412 d irrad. to 1×10^8 rad.

Carbon steel was attacked under all test conditions. There was no clear correlation between the presence of LOMI reagent and irradiation on the extent of attack. However, it was found that for all test conditions, the rate of initiation of corrosion "pock marks" with each test cycle tended to decrease. This could be connected with evaporation of moisture from the resins during specimen examination. Neither Type 304 nor Type 316 stainless steel suffered corrosion in the absence of irradiation. The presence of LOMI reagent did not make any difference for this non-irradiated condition. For the irradiated state, however, Type 316 stainless steel showed improved resistance to corrosion. This may be seen for as-received resins exposed to a gamma dose of 2.1×10^8 rad over a period of 447 d. Under these conditions, spot attack was noted for Type 304 but not for Type 316. If LOMI reagent was present on the resin, then both Type 304 and Type 316 showed spot attack after a 412 d irradiation to 1×10^8 rad. It seems clear that LOMI reagent encourages attack, at least for

Type 316 stainless steel, since in this case the cumulative gamma dose was only 1×10^8 rad.

TiCode-12 and Ferralium-255 are superior to all of the other metal specimens in terms of corrosion resistance. Neither showed attack under any of the test conditions studied.

Finally, high-density polyethylene did not show crack initiation or propagation in a gamma irradiation environment because of the rapid loss of oxygen to resin oxidation processes. This lack of oxygen is known to greatly retard oxidative degradation of polymers, as was mentioned above. When irradiation is absent, then sufficient oxygen remains in the test system to allow some crack initiation and propagation in both as-received and LOMI-loaded resins.

4. REFERENCES

Adams, J.W., and P. Soo, "The Impact of LWR Decontamination on Solidification, Waste Disposal and Associated Occupational Exposure, Annual Report," Brookhaven National Laboratory, NUREG/CR-3444, Vol. 5, June 1988.

Bowerman, B.S., and P.L. Piciulo, "Technical Considerations Affecting Preparation of Ion-Exchange Resins for Disposal," Brookhaven National Laboratory, NUREG/CR-4601, May 1986.

Davis, M.S., "The Impact of LWR Decontaminations on Solidification, Waste Disposal and Associated Occupational Exposure, Annual Report," Brookhaven National Laboratory, NUREG/CR-3444, Vol. 1, August 1983.

Davis, M.S., "The Impact of LWR Decontaminations on Solidification, Waste Disposal and Associated Occupational Exposure, Annual Report," Brookhaven National Laboratory, NUREG/CR-3444, Vol. 2, February 1985.

Gillen, K.T., and R.L. Clough, "Occurence and Implications of Radiation Dose Rate Effects for Material Aging Studies," Rad. Phys. Chem. 10, 679-687 (1981).

Helfferich, F., Ion-Exchange,McGraw-Hill, Inc., New York, 1962.

Kennedy, J.H., Analytical Chemistry, Harcourt Brace Jovanovich, Inc., New York, 1984.

NRC, "Technical Position on Waste Form", Rev. 0, 1983, contained in letter by L.B. Higginbotham to Commission Licensees entitled "Final Waste Classification and Waste Form Technical Position Papers," May 11, 1983.

Piciulo, P.L., and others, "The Impact of LWR Decontaminations on Solidification, Waste Disposal and Associated Occupational Exposure, Annual Report," Brookhaven National Laboratory, NUREG/CR-3444, Vol. 3, November 1985.

Piciulo, P.L., and J.W. Adams, "The Impact of LWR Decontaminations on Solidification, Waste Disposal and Associated Occupational Exposure, Annual Report," Brookhaven National Laboratory, NUREG/CR-3444, Vol. 4, October 1986.

Soo, P., and others, "The Effects of Environment and Gamma Irradiation on the Mechanical Properties of High Density Polyethylene," Brookhaven National Laboratory, NUREG/CR-4607, March 1986.

Terselius, B., V.W. Gedde, and J.F. Jansson, "Structure and Morphology of Thermally Oxidized High Density Polyethylene Pipe," Polymer Eng. and Sci., 22, 422 (1982).

APPENDIX A

BROOKHAVEN NATIONAL LABORATORY

MEMORANDUM

DATE: January 31, 1983

TO: File

FROM: B. S. Bowerman BSB

SUBJECT: **Elemental composition of ion-exchange resins IRN-77 and -78.**

In a telephone conversation on Friday, January 28, 1983, Mr. Charles Dicker of Rohm and Haas reported the elemental composition of the ion-exchange resins IRN-77 and IRN-78 as given in the table below. The figures for IRN-77 were calculated from data which he had and were based primarily on an exchange capacity of 5.0 $\pm$ 0.1 meq/g dry weight. Those for IRN-78 were also based on data which he had on IRA-400 (Cl^- form) from which IRN-78 is made. The IRA-400 has a dry weight exchange capacity of 4.0 $\pm$ 0.1 meq/g which translates to 4.3 meq/g for the OH^- form (IRN-78). The composition of the IRN-78 had to be calculated indirectly because its dry weight capacity cannot be measured directly. This is because IRN-78 loses its nitrogen functionality upon drying. Presumably this is due to the loss of NH_4OH as ammonia and water. The wet volumetric exchange capacities were given as 1.8 meq/ml for IRN-77 and 1.2 meq/ml for IRN-78 and the bulk densities of the wet resins (as delivered) are 50 lb/ft^3 and ~42.5 lb/ft^3, respectively. Mr. Dicker stated that the wet exchange capacities are the minimum specifications for manufacture.

Elemental Weight Percent Composition
of Dry Ion-Exchange Resins

Element	IRN-77	IRN-78
C	54	78
H	6	9
S	16	--
O	24	7
N	--	6

BSB:gfs
cc: M. S. Davis
R. Davis
L. Milian
J. Adams
C. Anderson
K. Swyler

NRC FORM 335 (2-89) NRCM 1102, 3201, 3202

U.S. NUCLEAR REGULATORY COMMISSION

BIBLIOGRAPHIC DATA SHEET

(See instructions on the reverse)

1. REPORT NUMBER (Assigned by NRC, Add Vol., Supp., Rev., and Addendum Numbers, if any.)

NUREG/CR-3444
BNL-NUREG-51699
Vol. 6

2. TITLE AND SUBTITLE

The Impact of LWR Decontaminations on Solidification, Waste Disposal and Associated Occupational Exposure

3. DATE REPORT PUBLISHED

MONTH: November
YEAR: 1989

4. FIN OR GRANT NUMBER

A3246

5. AUTHOR(S)

P. Soo, C.R. Kempf, K. Brumfield, L.W. Milian, J.W. Adams

6. TYPE OF REPORT

Annual

7. PERIOD COVERED (Inclusive Dates)

8. PERFORMING ORGANIZATION – NAME AND ADDRESS (If NRC, provide Division, Office or Region, U.S. Nuclear Regulatory Commission, and mailing address; if contractor, provide name and mailing address.)

Brookhaven National Laboratory
Upton, NY 11973

9. SPONSORING ORGANIZATION – NAME AND ADDRESS (If NRC, type "Same as above"; if contractor, provide NRC Division, Office or Region, U.S. Nuclear Regulatory Commission, and mailing address.)

Division of Engineering
Office of Nuclear Regulatory Research
U.S. Nuclear Regulatory Commission
Washington, DC 20555

10. SUPPLEMENTARY NOTES

11. ABSTRACT (200 words or less)

Studies were carried out to investigate if simulated decontamination reagent/resin waste combinations could give rise to thermal excursions during dewatering events. The results of temperature measurements and visual observations are given. In addition, the corrosion of various container materials in simulated decontamination resin waste was studied. In particular, the effects of gamma irradiation were quantified.

12. KEY WORDS/DESCRIPTORS (List words or phrases that will assist researchers in locating the report.)

low-level waste
decontamination waste
ion-exchange resin
corrosion
irradiation
waste container
resin degradation

13. AVAILABILITY STATEMENT

Unlimited

14. SECURITY CLASSIFICATION

(This Page) Unclassified

(This Report) Unclassified

15. NUMBER OF PAGES

16. PRICE

*U.S. G.P.O. 1989-262-436:00342

NUREG/CR-3444, Vol. 6

THE IMPACT OF LWR DECONTAMINATIONS ON SOLIDIFICATION, WASTE DISPOSAL AND ASSOCIATED OCCUPATIONAL EXPOSURE

NOVEMBER 1989